nature communications

Article

https://doi.org/10.1038/s41467-024-53651-1

Sugar transporter modulates nitrogen-determined tillering and yield formation in rice

Received: 15 February 2024

Accepted: 16 October 2024

Published online: 25 October 2024

Check for updates

Jinfei Zhang[1,2], Yuyi Zhang[1,2], Jingguang Chen[3], Mengfan Xu[1,2], Xinyu Guan[1,2], Cui Wu[4], Shunan Zhang[1,2], Hongye Qu[1,2], Jinfang Chu[5,6], Yifeng Xu[4], Mian Gu[1,2], Ying Liu[1,2] ✉ & Guohua Xu[1,2] ✉

Nitrogen (N) fertilizer application ensures crop production and food security worldwide. N-controlled boosting of shoot branching that is also referred as tillering can improve planting density for increasing grain yield of cereals. Here, we report that Sugar Transporter Protein 28 (OsSTP28) as a key regulator of N-responsive tillering and yield formation in rice. N supply inhibits the expression of *OsSTP28*, resulting in glucose accumulation in the apoplast of tiller buds, which in turn suppresses the expression of a transcriptional inhibitor *ORYZA SATIVA HOMEOBOX 15* (*OSH15*) via an epigenetic mechanism to activate gibberellin 2-oxidases (GA2oxs)-facilitated gibberellin catabolism in shoot base. Thereby, OsSTP28-OSH15-GA2oxs module reduces the level of bioactive gibberellin in shoot base upon increased N supply, and consequently promotes tillering and grain yield. Moreover, we identify an elite allele of *OsSTP28* that can effectively promote N-responsive tillering and yield formation, thus representing a valuable breeding target of N use efficiency improvement for agricultural sustainability.

Nitrogen (N) as an essential macronutrient largely determines crop yield in agricultural production[1]. Widespread adoption of high-yielding semi-dwarf gramineous crop varieties after green revolution in 1960s exhibit remarkably enhanced lodging resistance to elevated N fertilizer input which further drives farmers to supply N fertilizers for boosting yield[2,3]. However, excessive N fertilizer input causes huge energy cost and environmental risks, including soil acidification, water eutrophication, and greenhouse gas emission[4,5]. Thus, the identification of new genetic resources and elite germplasms with high N use efficiency (NUE) and key genes to enhance NUE becomes an important task for the genetic improvement of grain yield and NUE.

In rice production, grain yield is majorly determined by three agronomic traits: tiller number (also referred as panicle number), grain number per panicle, and grain weight. Due to the defect of gibberellin (GA) biosynthesis pathway in rice semi-dwarf varieties, the response of plant height is less sensitive to increased N supply, while boosting shoot branching/tillering becomes a more promising approach to improve yield under luxury N input condition[2,3]. Indeed, the enhancement of tillering makes a major contribution to the improvement of rice yield and NUE in response to increased N fertilizer input[6,7]. OsTCP19, encoding a TCP family transcription factor, plays a vital role in controlling the tillering response to N (TRN) in rice. Intriguingly, the elite allele *OsTCP19-H* with higher NUE is mostly distributed in wild rice but it has largely been lost in modern Asian cultivated rice[7]. However, most modern rice cultivars used after green revolution still exhibit a high sensitivity to boost tillering in response to increased N supply,

[1]State Key Laboratory of Crop Genetics & Germplasm Enhancement and Utilization, Nanjing Agricultural University, Nanjing 210095, China. [2]Key Laboratory of Plant Nutrition and Fertilization in Low-Middle Reaches of the Yangtze River, Ministry of Agriculture, Nanjing Agricultural University, Nanjing 210095, China. [3]School of Agriculture, Shenzhen Campus of Sun Yat-sen University, Shenzhen 518107, China. [4]College of Life Sciences, Nanjing Agriculture University, Nanjing 210095, China. [5]National Center for Plant Gene Research (Beijing), Institute of Genetics and Developmental Biology, Chinese Academy of Sciences, Beijing 100101, China. [6]University of Chinese Academy of Sciences, Beijing 100049, China. ✉e-mail: liuy@njau.edu.cn; ghxu@njau.edu.cn

indicating the existence of an OsTCP19-independent regulatory pathway to control N-responsive tillering in cultivated rice.

In rice, tiller originates from tiller bud at the axil of leaf, and in turn undergoes the outgrowth process to complete its development[8,9]. Tillering is a complex trait largely influenced by various environmental cues, especially by soil N availability[6]. Increased N supply boosts rice tiller number by promoting the outgrowth rather than the initiation of tiller buds, thus substantially improving effective panicle number to achieve higher grain yield[10,11]. External cues of N availability can be integrated into the internal tillering programming via modulating several phytohormone pathways, such as auxin, strigolactone (SL), and GA[6,11,12]. In particularly, GA functions as an inhibitor of tiller development[13,14]. N-mediated Tiller Growth Response 5 (NGR5), a downstream component of GA signaling pathway, is required for achieving N-induced tillering in rice. NGR5 is a target of GA receptor Gibberellin Insensitive Dwarf 1 (GID1), thus being stabilized by DELLA proteins. In response to elevated N supply, NGR5 recruits Polycomb Repressive Complex 2 (PRC2) to suppress the expression of several tillering inhibitors via H3K27 methylation, thereby promoting rice tillering and grain yield[11]. However, it is still unknown how rice integrates the signal of N availability into the GA-NGR5 module to regulate N-responsive tillering.

Here, we report the identification of a sugar transporter OsSTP28 as a key regulator of N-responsive tillering and yield formation in rice, and demonstrate that N supply represses the expression of *OsSTP28* to fine turn the level of apoplastic glucose in tiller buds, which in turn coordinates GA catabolism to boost tillering. In addition, we also identify an elite allele of *OsSTP28* that can more efficiently promote N-responsive tillering and yield formation in modern cultivated rice varieties, thus providing a valuable germplasm for the genetic improvement of yield and NUE in rice.

Results

Os*STP28* is associated with tillering response to N in rice

To explore the genetic basis of TRN, we employed a rice multiparent advanced generation intercross (MAGIC) population that was developed by four-way cross of four elite rice varieties with a high range of genetic diversity[15] (Fig. 1a–c). Firstly, we evaluated the variation of TRN in four parental varieties in paddy field supplied with low N (LN, 150 kg ha^{-1}) or high N (HN, 350 kg ha^{-1}). Tiller number of two varieties HHZ5-SAL9-Y3-Y1 (HH) and PR33282-B-8-1-1-1-1-1 (PR) were substantial increased by improved N input, while the tillering response in the other two varieties SAGC-08 (SA) and BP1976B-2-3-7-TB-1-1 (BP) were insensitive to the changed N availabilities (Fig. 1a, b). The diverse TRN among parental varieties makes it possible to identify the genetic determinant of N-regulated tillering in this MAGIC population. Next, we measured the tillering trait in this MAGIC panel consisting of 120 lines (Fig. 1c) under both LN and HN conditions, and observed a high degree of phenotypic variation in the tiller number range and response to N (Fig. 1d, e). By performing a GWAS analysis, we identified a genetic locus at chromosome 11 with a group of single nucleotide polymorphisms (SNPs) highly associated with the tiller number under HN condition, and the most significantly associated SNP ($-\log_{10}(P) = 5.20$) is located at chromosome 11: 22627320 (Fig. 1f). This linkage disequilibrium (LD) block spans an approximately 30-kb region containing five candidate genes (Fig. 1f).

To ascertain the causal gene for the associated locus, we selected 18 MAGIC lines with contrasting TRN and assessed the transcriptional expression pattern of all five candidate genes in shoot base under different N supplies. As shown, only *Os11g0594000 (OsSTP28)* displayed a N-responsive expression pattern. Specifically, the transcriptional expression level of *OsSTP28* was remarkably repressed by improved N supply in high TRN lines, by contrast the expression response of *OsSTP28* was insensitive to the changed N input in low TRN lines (Fig. 1g). Notably, among all five candidate genes, only *OsSTP28* exhibited a negative correlation between the expression response to N (ERN) and TRN under different N supplies (Fig. 1h; Supplementary Fig. 1), suggesting *OsSTP28* is likely the causal gene leading to the natural variation of TRN in the MAGIC population.

We further dissected the genetic feature of associated locus with TRN by conducting a haplotype analysis of *OsSTP28* in MAGIC population. It showed that the nucleotide polymorphism (two InDels are located at chromosome 11: 22624546 and 22625579, respectively) causing the variation of TRN were located in the promoter region of *OsSTP28* (Fig. 1i), while no substitution was found in its coding DNA sequence (CDS). We classified the tested MAGIC population into two groups according to the *OsSTP28* haplotype distribution (Fig. 1i), and MAGIC lines containing *OsSTP28* haplotype H (high response to N) allele displayed a higher sensitivity of TRN than those lines with *OsSTP28* haplotype C (common response to N) allele (Fig. 1j, k). This result confirmed that *OsSTP28* is the causal gene determining the genetic diversity of N-induced tillering in rice.

To dissect the mechanism why *OsSTP28*$^{Hap.\ H}$ allele is more sensitive to N supply, we performed a cis-acting element analysis by scanning the promoter regions of *OsSTP28*$^{Hap.\ C}$ and *OsSTP28*$^{Hap.\ H}$. Interestingly, a CCA1/Nhd1 (circadian regulator) binding element[16,17] and a NLP3 (N signaling regulator) binding element[18,19] were identified nearby the polymorphic site P1 and P2, respectively (Supplementary Fig. 2a), indicating these two SNPs in the promoter region of *OsSTP28* are likely to influence the rhythmic and N-responsive expression pattern of *OsSTP28*. Next, by transient dual-luciferase assays in rice protoplast, we found that introducing P2$^{Hap.\ H}$ (Hap.C_{p2H}) rather than P1$^{Hap.\ H}$ (Hap.C_{p1H}) to *OsSTP28*$^{Hap.\ C}$ promoter endowed *OsSTP28* with a higher sensitivity to N supply (Supplementary Fig. 2b, c). Moreover, we found that several representative MAGIC lines containing P2$^{Hap.\ H}$ in *OsSTP28* promoter exhibited higher sensitivities to N compared with those lines with P1$^{Hap.\ H}$ sequence (Supplementary Fig. 2d, e). These results revealed that the polymorphic site P2 with 2-bp indel in *OsSTP28*$^{Hap.\ H}$ promoter is critical to control the transcriptional response of *OsSTP28* to N supply in rice.

To address the question whether *OsSTP28* alleles had been selected during rice domestication, we screened *OsSTP28* haplotype information among 4726 rice accessions by the algorithm of RiceVarMap v2.0[20], and found that *OsSTP28*$^{Hap.\ H}$ allele existed in 78.2% of *indica* rice varieties, 76.6% of *japonica* rice varieties, 85.4% of *intermediate* rice varieties, and 40.4% of *aus* rice varieties (Supplementary Fig. 3). The frequencies of *OsSTP28*$^{Hap.\ H}$ allele occurrence are nearly equivalent in *indica* and *japonica* rice, implying that *OsSTP28* might be involved in a conservative regulatory pathway that widely exists across modern Asian cultivated rice and ensures the adaptation of tillering to the fluctuating N availabilities.

OsSTP28 acts as a repressor of N-dependent tillering in rice

Next, we assessed the expression pattern of *OsSTP28* in rice. Quantitative reverse transcription polymerase chain reaction (qRT-PCR) assay showed that *OsSTP28* is preferentially expressed in shoot base and slightly expressed in leaf blades of rice seedlings (Supplementary Fig. 4a). In agreement with this, histochemical analysis of *proOsSTP28:GUS* reporter lines revealed that *OsSTP28* is highly expressed in axillary buds with minor expression in adventitious root primordia and vascular tissue of leaves (Supplementary Fig. 4b). Further, in situ hybridization analysis also confirmed that *OsSTP28* is preferentially expressed in the axillary bud (Fig. 2a), indicating a possible function of OsSTP28 in tiller development. Moreover, *OsSTP28* expression level was induced by N deficiency and repressed by N supply no matter in the forms of NH_4^+, NO_3^-, or NH_4NO_3 (Fig. 2b), indicating that *OsSTP28* transcript abundance is determined by N status in seedlings. Indeed, the supply of organic N form glutamine (Gln) also significantly inhibited the expression of *OsSTP28* (Fig. 2b). Consistently, when N assimilation was blocked by the supplementation

https://doi.org/10.1038/s41467-024-53651-1

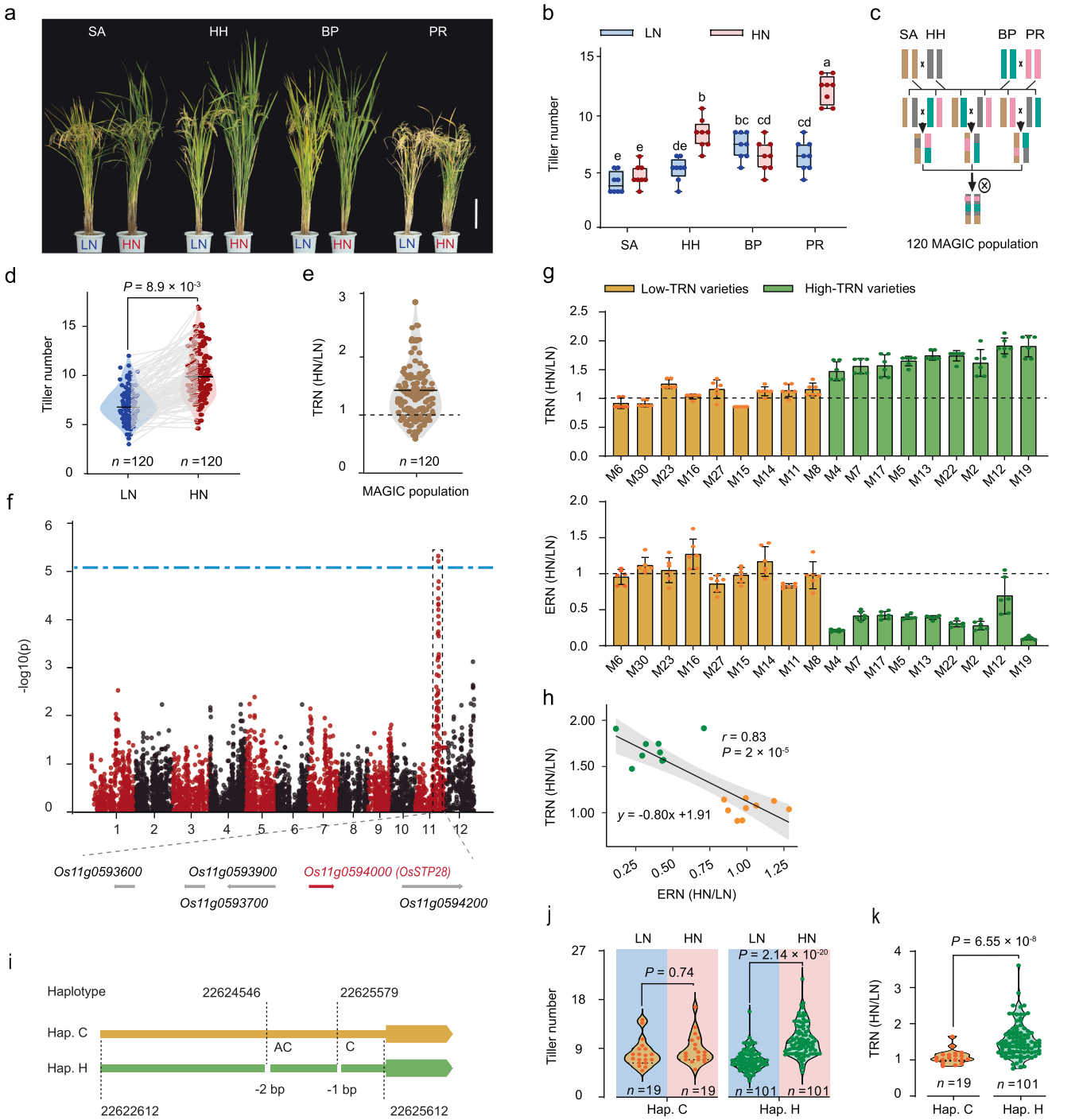

Fig. 1 | *OsSTP28* locus is associated with tillering response of rice to N supply. **a** Phenotype of four parent lines, SAGC-08 (SA), HHZ5-SAL9-Y3-Y1 (HH), BP1976B-2-3-7-TB-1-1 (BP) and PR33282-B-8-1-1-1-1-1(PR), of rice MAGIC population under low nitrogen (LN) or high nitrogen (HN) supply at mature stage. White bars, 20 cm. **b** Tiller number per plant of four parent varieties under LN or HN supply. Boxes show the first quartile, median, and third quartile; whiskers show the minimum and maximum values. $n = 8$ individual plants. Different letters indicate significant differences among the treatments ($P < 0.05$, one-way ANOVA, Tukey's HSD test). **c** Pattern diagram of MAGIC population construction by four parents. **d** Tiller number of 120 MAGIC accessions under LN or HN supply. The dots represent the accessions, lines connect the same accession under LN or HN supply. **e** Variation of tillering response to N (TRN, the ratio of tiller number between HN and LN). **f** Manhattan plot for the associations of single nucleic acid polymorphism (SNP) to tiller number under HN on rice whole genome, and the position of 5 candidate genes on rice chromosome 11. Negative $\log_{10}$-transformed *P*-values from a genome-wide scan were plotted against positions on each of the 12 chromosomes of rice (*Oryza sativa* L). **g** TRN and expression response to N (ERN) of *OsSTP28*. **h** Correlation between TRN and ERN. The data used for the correlation analyses derived from experiments shown in Fig. 1g. **i** Natural allelic variation at the promoter region of *OsSTP28* in the MAGIC population. The haplotype is referred to as haplotype C (tillering common-response to N, containing 19 lines including SA and BP), and haplotype H (tillering high-response to N, containing 101 lines including HH and PR). Number in yellow or green denotes the number of lines carrying the corresponding allele. **j** Tiller number of MAGIC lines representing two *OsSTP28* haplotypes under LN or HN supply at mature stage. **k** TRN (HN/LN) of two haplotype lines of MAGIC population. The data used for calculation of TRN derived from experiments shown in Fig. 1j. Significant difference was determined by two-sided Student's *t*-test in **d**, **j** and **k**.

https://doi.org/10.1038/s41467-024-53651-1

of methionine sulfoximine (MSX), an inhibitor of glutamine synthetase, the inhibitory effect of N on *OsSTP28* transcription was largely alleviated (Supplementary Fig. 4c). These results revealed that *OsSTP28* expression is negatively regulated by internal N status in rice. Altogether, the tiller bud localization and N-responsive expression pattern strongly suggested an involvement of *OsSTP28* in the regulation of N-determined tillering in rice.

To explore the function of *OsSTP28* in tillering, three independent *OsSTP28* knockout mutants (*stp28-1*, *stp28-2* and *stp28-3*) were generated in the background of Nipponbare (NIP) by CRISPR/Cas9 technology (Supplementary Fig. 5a). Knockout of *OsSTP28* remarkably stimulated the outgrowth of tiller buds (Supplementary Fig. 5b–d). Consistently, in paddy field, *stp28* knockout lines also generated more tillers than WT after 6 weeks of transplanting under LN or HN supply (Fig. 2c, d). At the ripening stage (11 weeks after transplanting), tiller number in *stp28* mutant lines was increased by ~49% under LN supply and by ~35% under HN condition compared with that in WT (Fig. 2c, d), suggesting that OsSTP28 is a repressor of tillering in rice. Additionally,

Fig. 2 | Axillary bud located *OsSTP28* negatively regulates tillering response of rice to N. a In situ hybridization of *OsSTP28* mRNA in tiller buds. Scale bar, 100 nm. **b** Relative expression of *OsSTP28* responding to different forms and concentrations of N. *OsActin1* was used as an internal standard. Data are mean ± SD ($n = 4$ biological replicates). **c** Phenotype of WT and *stp28* mutants under LN or HN supply. Scale bar, 20 cm. **d** Tiller number of WT and *stp28* lines at different growth stage under LN or HN supply. Data are mean ± SD ($n = 7$ individual plants). **e** Tillering response to N of WT and *stp28* lines at different developmental stage. Data are mean ± SEM ($n = 7$ individual plants). In (**d**, **e**), asterisks denote significant differences between WT and indicated lines at $^*P < 0.05$ and $^{**}P < 0.01$ by Dunnett's multiple tests. **f** Schematic of transgenic constructs used for the complementation of *stp28-3* mutant by expressing *OsSTP28(NIP)* coding sequence under the control of the different promoters ($CS_{Hap.C}$, *proOsSTP28* of SA; $CS_{Hap.H}$, *proOsSTP28* of HH). **g** Representative photographs of WT, *stp28-3*, CS_{NC}, $CS_{Hap.C}$ and $CS_{Hap.H}$ under LN or HN supply. CS_{NC} is a negative control with empty vector. Scale bar, 20 cm. *OsSTP28* expression abundance (**h**) and Tiller number (**i**) in WT, *stp28-3*, CS_{NC}, $CS_{Hap.C}$ and $CS_{Hap.H}$ under LN or HN supply. *OsActin1* was used as an internal standard. Four independent $CS_{Hap.C}$ and $CS_{Hap.H}$ complementation lines were tested in this study. Accordingly, in (**h**), data are mean ± SD ($n = 3$ biological replicates for WT, *stp28-3*, and CS_{NC}; $n = 12$ biological replicates for $CS_{Hap.C}$ and $CS_{Hap.H}$). In (**i**), data are mean ± SD ($n = 5$ individual plants for WT, *stp28-3*, and CS_{NC}; $n = 20$ individual plants for $CS_{Hap.C}$ and $CS_{Hap.H}$). **j** The correlation between tillering number and *OsSTP28* expression level of WT, *stp28-3*, CS_{NC}, $CS_{Hap.C}$ and $CS_{Hap.H}$. **k** TRN of WT, *stp28-3*, CS_{NC}, $CS_{Hap.C}$ and $CS_{Hap.H}$. Data are mean ± SD ($n = 5$ biological replicates for WT, *stp28-3*, and CS_{NC}; $n = 20$ biological replicates for $CS_{Hap.C}$ and $CS_{Hap.H}$). In (**b**, **h**, **i**, **j**, **k**), different letters indicated significant differences ($P < 0.05$, one-way ANOVA, Tukey's HSD test).

to evaluate whether TRN in rice depends on the action of *OsSTP28*, we calculated the ratio of tiller number between HN and LN conditions in WT and *stp28* mutants. It showed that tillering response in *stp28* mutants became less sensitive to N supply than that in WT (Fig. 2e). Therefore, our data demonstrate that OsSTP28 is a negative regulator of tillering and required for achieving tillering response to N in rice.

Considering that allelic variation of *OsSTP28* that occurs in its promoter is the cause of TRN diversity in rice, we conducted a promoter swapping experiment to verify the differential effect of $OsSTP28^{Hap.H}$ and $OsSTP28^{Hap.C}$ alleles on N-dependent tillering. For this purpose, we complemented *stp28-3* mutant with *OsSTP28* coding sequence (cloned from NIP variety) driven by the promoter of $OsSTP28^{Hap.H}$ or $OsSTP28^{Hap.C}$ allele (Fig. 2f). The complementary construct of *OsSTP28* alleles recovered the expression of *OsSTP28* in *stp28* mutant, but interestingly $OsSTP28^{Hap.H}$ allele was responsive to N supply at transcriptional level whereas $OsSTP28^{Hap.C}$ was nearly insensitive to N under the same condition (Fig. 2h). Accordingly, the complementation of *OsSTP28* alleles recovered tiller development in *stp28* mutant, but $OsSTP28^{Hap.H}$ rather than $OsSTP28^{Hap.C}$ allele endowed *stp28* mutant with the ability to achieve N-induced tillering to the similar extent as wild-type (Fig. 2i). The significantly negative correlation between *OsSTP28* transcript abundance and tiller number among all these lines highly suggested that the expression level of *OsSTP28* determines TRN (Fig. 2j), and in addition, $OsSTP28^{Hap.H}$ allele exhibited a higher sensitivity of TRN than that of $OsSTP28^{Hap.C}$ allele (Fig. 2k). Thereby, we conclude that $OsSTP28^{Hap.H}$ is an elite allele to regulate TRN in rice.

OsSTP28 encodes an influx hexose transporter coordinating N-mediated rhythmic fluctuation of glucose in rice

Sugar Transporter Protein (STP) is a prominent member of monosaccharide transporter family in plants[21]. Here, OsSTP28 is predicated as a STP member in rice (Supplementary Fig. 6a). To verify the function of OsSTP28 as a hexose transporter, we assessed its subcellular localization in rice protoplast and its activity in transporting different forms of hexose in yeast cells. The results show that OsSTP28 is a plasma membrane localized protein (Fig. 3a) and exhibits higher capacity to transport glucose, lower capacity to transport mannose and galactose, and no activity in transport of fructose (Supplementary Fig. 7a). ^{13}C-glucose uptake experiment conducted in yeast (Fig. 3b) and in *Xenopus laevis* oocyte (Fig. 3c, d) further revealed that OsSTP28 mediates glucose influx rather than efflux. Moreover, kinetic analysis of ^{13}C-glucose showed that OsSTP28 facilitates high affinity glucose uptake with a $K_m = 76.15 \pm 5.54$ μM (Supplementary Fig. 7b). Taken together, our data demonstrate that OsSTP28 is a plasma membrane-localized hexose transporter responsible for glucose influx.

Next, we addressed the question whether OsSTP28 impacts sugar status or distribution in the shoot base where the tiller is initiated. Interestingly, *OsSTP28* expression in the shoot base displayed a strong rhythmic pattern, which peaked in the night and troughed in the day (Fig. 3e). Under the same condition, sugars in WT and *stp28* mutants also exhibited the rhythmic fluctuations with sucrose peaked at dusk and troughed at dawn. Notably, glucose peaked at middle of daytime, troughed at the onset of night phase. Both glucose and fructose increased during night (Fig. 3f). Particularly, rather than sucrose and fructose, the status of glucose was most significantly influenced by the knockout of *OsSTP28* representing as an enhancement of glucose over the night period without altering the phase of its diel oscillation (Fig. 3f). These data revealed a vital role of OsSTP28 in modulating glucose status of the shoot base at night.

Then, we detected the effect of OsSTP28 on N-mediated sugar distribution in the shoot base. The level of glucose and fructose in the shoot base was elevated in the night and reduced in the day, while sucrose exhibited an opposite trend (Supplementary Fig. 8a), supporting the common observation that sucrose is enzymatically hydrolyzed to glucose and fructose for the respiration to maintain plant growth in the evening[22]. Elevated N supply increased both sucrose and glucose of WT at day and/or night. Compared with WT, knockout of *OsSTP28* led to a remarkable accumulation of glucose, but not sucrose or fructose, in the shoot base at night irrespective of N supply level (Supplementary Fig. 8a). ^{13}C-glucose feeding experiment further revealed that the blade-to-shoot base glucose translocation was enhanced by N supply in WT, and significantly improved by the knockout of *OsSTP28* (Supplementary Fig. 8b). Since *OsSTP28* expression was repressed by N supply (Fig. 2b), we assumed that N-induced glucose accumulation in shoot base was likely due to the down-regulation of *OsSTP28*, and thereby *OsSTP28* inactivation further elevated the accumulation of glucose in the shoot base. This hypothesis was verified by the experiment that complementation of *OsSTP28* expression in *stp28* mutant recovered the concentration of both endogenous and external ^{13}C-labelled glucose in the shoot base to the same extent as WT, especially driven by the promoter of elite $OsSTP28^{Hap.H}$ allele (Supplementary Fig. 8c, d).

We further addressed the question how OsSTP28 impacts sugar distribution associated with tillering development. Given that OsSTP28 facilitates glucose influx on plasma membrane, we hypothesized that down-regulation or knockout of *OsSTP28* would lead to an accumulation of glucose in the apoplast. Indeed, apoplastic glucose level in shoot base was increased by HN supply in WT, and this accumulation of apoplastic glucose was further dramatically enhanced by knockout of *OsSTP28* irrespective of N conditions (Fig. 3h). Notably, the change of apoplastic glucose between LN and HN supplies or between WT and *stp28* mutants was observed only at night not at the daytime. Meanwhile, no significant difference of apoplastic sucrose or fructose was observed between WT and *stp28* mutants (Fig. 3g, h). By contrast, intracellular sugar concentration, no matter for sucrose, glucose or fructose, did not show significant difference between WT and *stp28* mutants (Supplementary Fig. 9). Altogether, our study demonstrates that OsSTP28 plays a critical role in regulating the N-responsive rhythmic change of apoplastic glucose in rice shoot base.

https://doi.org/10.1038/s41467-024-53651-1

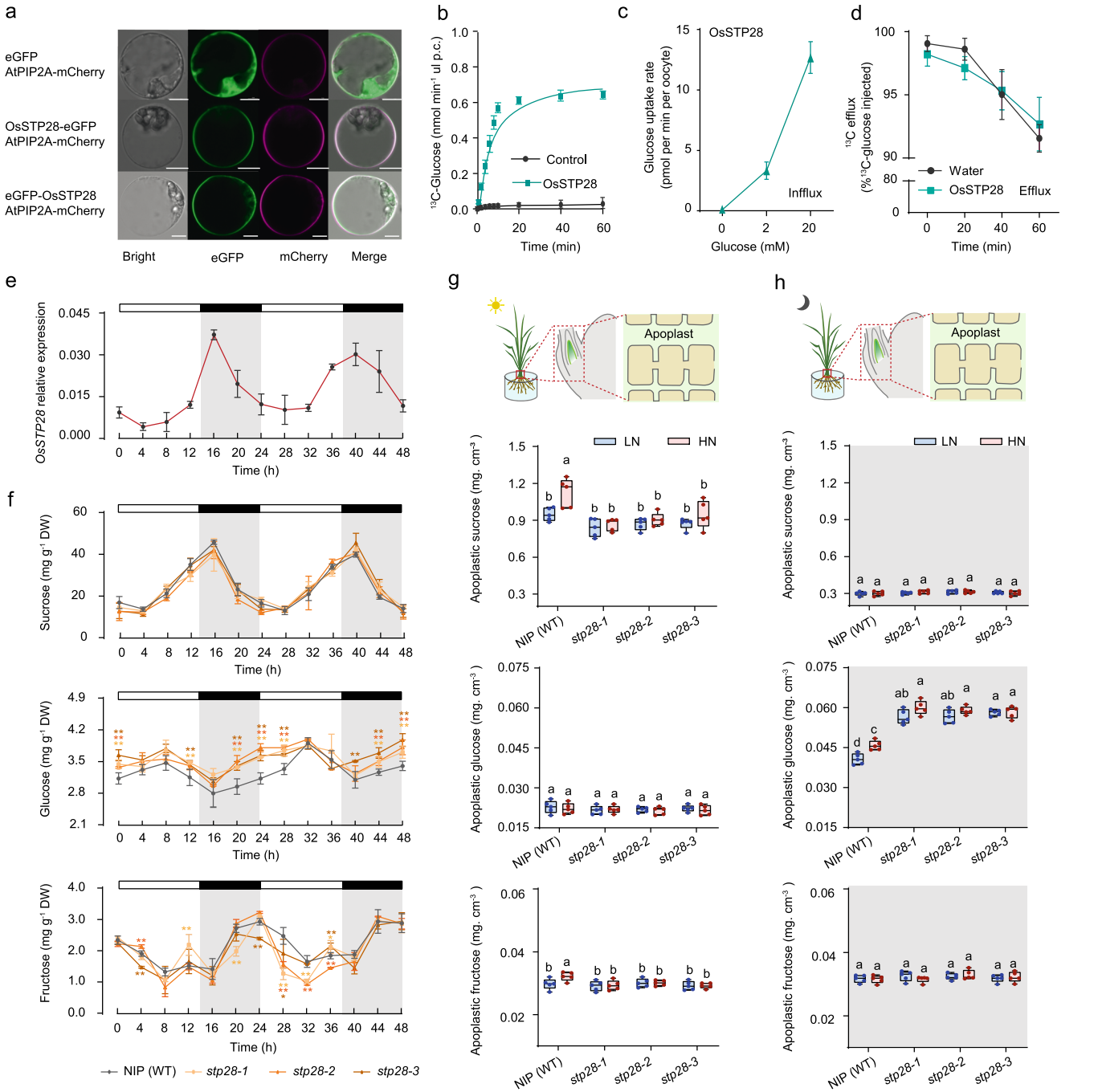

Fig. 3 | OsSTP28 as a plasma membrane localized hexose transporter controls N-dependent glucose accumulation at night in apoplast of shoot base. **a** Subcellular localization of OsSTP28-eGFP and eGFP-OsSTP28 fusion proteins in rice protoplasts. Scale bars, 10 μm. The results are representative of three independent experiments. **b** [^{13}C]-glucose transport capacity of OsSTP28 in yeast mutant strain EBY.VW4000. Yeast strains expressing OsSTP28-cDNA or an empty vector were cultured on 100 mM of glucose at pH 5.5. **c** Glucose influx assay in oocytes. The oocytes were exposed to MBS solution containing 0, 2, 20 (mM) glucose for 2 h, then washed and extracted with H_2O. **d** Glucose efflux assay in oocytes. [^{13}C]-glucose were injected into oocytes and transferred to fresh MBS for 2 h. The external solution was collected after 2 h. In **b**–**d**, data are mean ± SD (in **b** and **c**, $n = 5$ biological replicates; in (**d**), $n = 3$ biological replicates). **e** Diurnal rhythmic expression of *OsSTP28* in shoot. Data are mean ± SD ($n = 4$ individual seedlings). The samples were collected every 4 h for 2 d. The white and black bars represent light and dark conditions, respectively. **f** Sucrose, glucose and fructose concentrations in the shoot of WT and *stp28* lines. Data are mean ± SD ($n = 4$ biological replicates). Asterisks denote significant differences between control and indicated treatments at each time point as $^*P < 0.05$ $^{**}P < 0.01$ according to Dunnett's multiple test. **g**, **h** Apoplastic sucrose, glucose and fructose concentrations in shoot base of WT and *stp28* lines at the end of the day (**g**) and at end of the night (**h**) in response to N supply. Apoplastic solution was collected by centrifugation of the cells from WT and *stp28* mutants, which grown in LN or HN supply respectively for 35 d, calculated with apoplast hydration calculation method and measured by UPLC. Boxes show the first quartile, median, and third quartile; whiskers show the minimum and maximum values. $n = 5$ biological replicates. Different letters indicate significant differences ($P < 0.05$, one-way ANOVA, Tukey's HSD test).

Since *OsSTP28* is also slightly expressed in leaf blade, we further monitored apoplastic sugar status in leaves. The change of apoplastic sugar in leaf blade exhibited the same trend as that in shoot base. Specifically, at night, apoplastic glucose in leaf blade was also enhanced by N supply in WT, and the level of apoplastic glucose was elevated in *stp28* mutants compared with that in WT irrespective of N condition (Supplementary Fig. 10). Since N supply or knockout of *OsSTP28* improved blade-to-shoot base glucose translocation (Supplementary Fig. 8b), OsSTP28-depedent accumulation of apoplastic glucose in leaves might contribute to establish the glucose pool nearby axillary buds which is critical for stimulating tillering in rice.

OsSTP28 coordinates gibberellin metabolism to regulate tillering response to N

To uncover the molecular mechanism underlying OsSTP28-regulated TRN in rice, we performed RNA-sequencing (RNA-seq) analysis of shoot base between WT and *stp28* mutant under LN and HN supplies. A large number of differentially expressed genes (DEGs) between WT and *stp28* mutant (LN condition: 2466 DEGs; HN condition: 1744 DEGs) were identified (Supplementary Fig. 11a, b; Supplementary Data 1). Among them, many previously characterized tillering regulatory genes were differentially expressed between WT and *stp28* mutant and affected by N supplies. For instance, positive tillering regulators (*MOC1*, *OsMASD57*) were significantly up-regulated in *stp28* mutant, while negative tillering regulators (*OsTB1*, *OsSPL14*) were down-regulated in *stp28* mutant in comparison to WT[23–26] (Supplementary Fig. 12–13; Supplementary Data 2). The expression patterns of these tillering regulators were in well agreement with the enhanced tillering phenotype in *stp28* mutant compared with WT under both LN and HN supplies (Fig. 2c, d).

Gene ontology (GO) enrichment analysis of DEGs (*stp28* mutant *vs* WT) under LN and HN conditions further revealed that many biological processes relating to carbohydrate metabolism, glucose metabolism, carbon fixation, and organ growth were affected by the knockout of *OsSTP28* (Supplementary Fig. 11c; Supplementary Data 3), consistent with the elevated apoplastic glucose accumulated in the shoot base of *stp28* mutant (Fig. 3h).

Remarkably, GO enrichment analysis indicated that several GA metabolic processes were enriched among the DEGs (*stp28* mutant *vs* WT) under different N supplies (Supplementary Fig. 11c). Gene set enrichment analysis (GSEA) further highlighted that GA catabolism process was activated by the knockout of *OsSTP28* in rice under both LN and HN conditions (Supplementary Fig. 11d; Supplementary Data 4). Accordingly, the transcript abundances of a group of *GA2-oxidases* (*OsGA2ox3*, *OsGA2ox5*, *OsGA2ox8* and *OsGA2ox9*) that catalyze GA catabolism in rice were remarkably increased in *stp28* mutant compared with WT irrespective of N supply conditions (Fig. 4a; Supplementary Fig. 11e, f). In agreement with the expression pattern of *GA2-oxidases*, the GA2-oxidase enzymatic activity was increased in *stp28* mutants compared with WT (Fig. 4b). Since GA2-oxidase catalyzes the deactivation of bioactive GAs (GA_1 and GA_4) to generate catabolic GAs (GA_8 and GA_{34}) in plants[27], we assumed that the activation of GA2-oxidases in *stp28* mutants might change GA status. Indeed, bioactive GA_1 level was reduced in the shoot base of *stp28* mutants compared with WT, while catabolic GA_8 level was increased at the same situations (Fig. 4d). Besides, bioactive GA_4 and its catabolic form GA_{34} were too litter to be detected in our conditions (Supplementary Fig. 14). Meanwhile, in WT rice, increased N supply also enhanced the expression of *OsGA2ox3/5/8* and the enzymatic activity of GA2-oxidases, thus leading to a reduction of bioactive GA level in the shoot base (Fig. 4a–d). These results demonstrate that increasing N supply or knockout of *OsSTP28* reduces bioactive GA level via stimulating GA catabolism in rice, suggesting a vital role of OsSTP28 in the modulation of N-responsive GA metabolism.

Since GA acts as a repressor of N-responsive tillering in rice[11], we further investigated the relationship between OsSTP28 and GA metabolism in tillering regulation. *OsGA2ox5* had a highest transcript abundance among four OsSTP28-regulated GA2-oxidases (Fig. 4a; Supplementary Fig. 11f). Thus, we generated the knockout mutants of *OsGA2ox5* (*ga2ox5-1, ga2ox5-2, and ga2ox5-3*) by CRISPR/Cas9 system (Supplementary Fig. 15a). As expected, knockout of *OsGA2ox5* substantially reduced GA2-oxidases enzyme activity in shoot base (Fig. 4f), which was supposed to cause an over-accumulation of bioactive GA in seedlings. Correspondingly, tiller number and TRN were repressed by knockout of *OsGA2ox5* in rice (Fig. 4e–g). More importantly, we found that the enhanced tillering phenotype of *stp28* mutant was completely abolished in *stp28/ga2ox5* double mutant, suggesting that OsSTP28 functions genetically upstream of GA2-oxidase to regulate N-responsive tillering. Since NGR5 is a downstream component of GA pathway, NGR5 promotes N-responsive tillering by suppressing the expression of several tillering inhibitory genes, e.g. OsSPL14, D14[11]. By generating two *ngr5* mutants and a double mutant of *stp28/ngr5* in NIP background, we found that *stp28/ngr5* displayed a highly inhibited N-responsive tillering phenotype nearly the same as that of *ngr5* single mutant rather than *stp28* mutant (Supplementary Fig. 16), indicating that OsSTP28 functions genetically upstream of NGR5 as well. Taken together, our study demonstrates that OsSTP28 mediates a regulatory event that functions upstream of GA metabolism and NGR5 pathway to modulate N-dependent tillering in rice.

OSH15 is critical for OsSTP28-regulated gibberellin catabolism and tillering response to N

Since OsSTP28-regulated GA catabolism was achieved by altering *OsGA2oxs* expression at transcriptional level, we supposed that a transcription factor is required for this process. By data mining in the RNA-seq results, a *knotted1*-like homeobox (KNOX) transcription factor, *Oryza sativa homeobox 15* (*OSH15*) was identified as the most sensitive DEG between *stp28* mutant and WT under both LN and HN conditions (Fig. 5a). Specifically, *OSH15* expression was dramatically declined in *stp28* mutant compared with WT (Fig. 5b). Since the promoter of most GA2-oxidase genes including *OsGA2ox3, OsGA2ox5, OsGA2ox8, and OsGA2ox9* present TGAC motifs, a conserved KNOX binding site (Fig. 5c), OSH15 might be directly involved in the OsSTP28-regulated GA catabolism. Electrophoretic mobility shift assay (EMSA) revealed that OSH15 directly bound to the promoters of *OsGA2ox3, OsGA2ox5, OsGA2ox8, and OsGA2ox9* (Fig. 5c), thus resulting in a strong inhibition effect of OSH15 on the expression of *OsGA2ox3, OsGA2ox5, OsGA2ox8, and OsGA2ox9* (Fig. 5d).

To further investigate the function of OSH15 in GA metabolism and tillering, we generated *osh15* mutant lines by CRISPR/Cas9 system (Supplementary Fig. 15b). As expected, the expression of *OsGA2ox3, OsGA2ox5, OsGA2ox8, and OsGA2ox9* as well as the activity of GA2-oxidase were largely enhanced by the knockout of *OSH15* (Fig. 5e, f), and correspondingly tillering was also remarkably stimulated in the *osh15* mutants (Fig. 5g, h), fully mimicking the phenotype of *stp28* mutants. These results suggested that OSH15 makes a major contribution to achieve the influence of OsSTP28 on GA catabolism and tillering via inhibiting the transcription of *OsGA2oxs*. In agreement with this point, the complementation of *OsSTP28* in *stp28* mutant, especially $OsSTP28^{Hap.\ H}$ allele, recovered the expression of *OSH15* and *OsGA2oxs* as well as the activity of GA2-oxidase to the same extent as WT (Supplementary Fig. 17a, c), confirming that OSH15 functions downstream of OsSTP28 to regulate GA catabolism and tillering in rice. Moreover, *OSH15* expression is inhibited by elevated N supply in WT rice (Fig. 5b), and the responses of GA catabolism and tillering to N supply in *osh15* mutants were insensitive to the changed N inputs compared with WT (Fig. 5e–h), revealing a vital role of OSH15 in modulating N-responsive tillering in rice.

https://doi.org/10.1038/s41467-024-53651-1

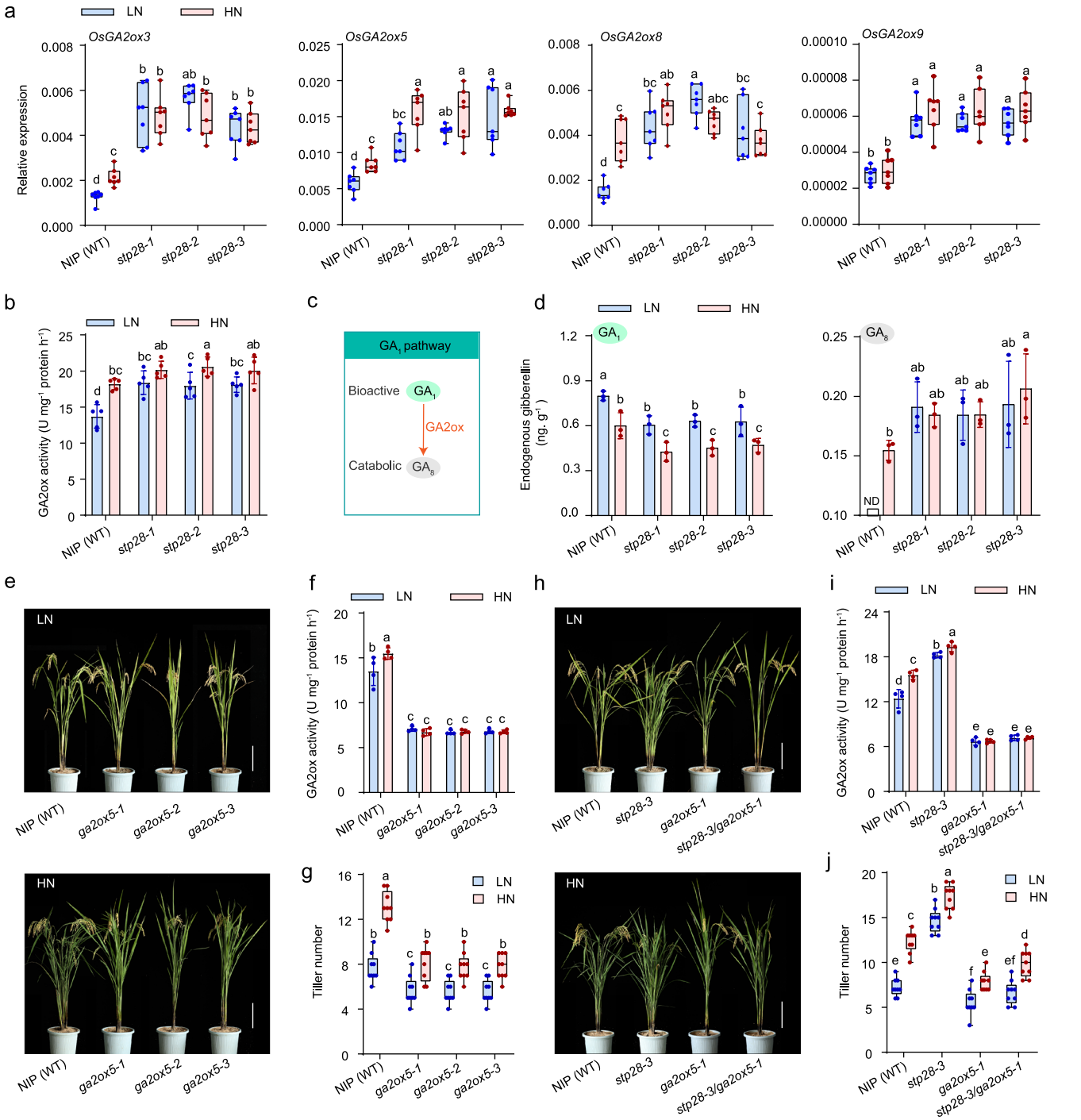

Fig. 4 | OsSTP28 functions upstream of GA2-oxidase mediated gibberellin metabolism pathway. a Expression abundance of *OsGA2ox3/5/8/9* in WT and *stp28* mutants under LN or HN supply. *OsGA2ox3/5/8/9* expression were assessed in shoot bases by qRT-PCR and normalized by *OsActin1*. Boxes show the first quartile, median, and third quartile; whiskers show the minimum and maximum values. $n = 7$ individual plants. **b** Gibberellin 2-oxidase (GA2ox) activities at shoot base of WT and *stp28* lines under LN or HN supply. The shoot bases of 35-d-old rice seedlings (WT and *stp28* lines) were collected for extracting GA2ox. Data are mean ± SD ($n = 5$ individual plants). **c** Schematic representation of the GA2ox catabolic pathway in higher plants. Bioactive GA_1 (marked with green background) was inactivated to GA_8 (marked with gray background) by GA2ox. **d** Comparison of the levels of two GA isoforms between WT and *stp28* lines under LN or HN supply. ND not detected. Data are mean ± SD ($n = 3$ individual plants). **e**–**g** Phenotype (**e**), GA2ox activities (**f**) and tiller number (**g**) of WT and *ga2ox5* lines under LN or HN supply. Scale bar, 20 cm. **h**–**j** Phenotype (**h**), GA2ox activities (**i**) and tiller number per plant (**j**) of WT, *stp28-3*, *ga2ox5-1*, and *stp28-3/ga2ox5-1* double mutant plants under LN or HN supply. Scale bar, 20 cm. Data in (**f**, **i**) represent mean ± SD ($n = 4$ biological replicates). In (**g**, **j**), boxes show the first quartile, median, and third quartile; whiskers show the minimum and maximum values. $n = 9$ individual plants. In (**a**, **b**, **d**, **f**, **g**, **i**, **j**), Different letters indicated significant differences ($P < 0.05$, one-way ANOVA, Tukey's HSD test).

https://doi.org/10.1038/s41467-024-53651-1

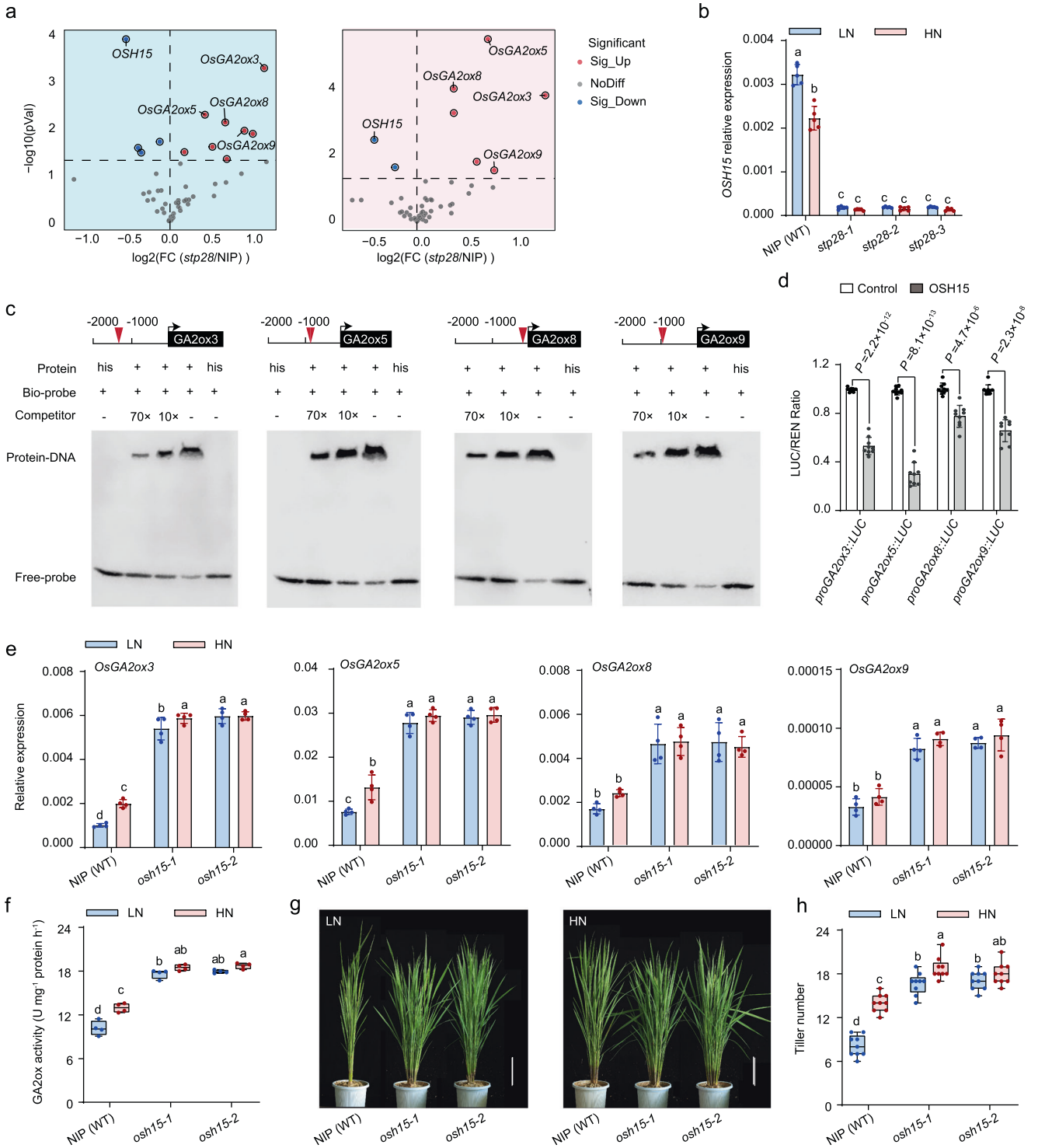

Fig. 5 | OSH15, a transcriptional inhibitor, is required for OsSTP28-regulated gibberellin catabolism. a Volcano plot of DEGs (the marker genes of tiller development) based on RNA-seq data from WT and *stp28* mutant (*stp28-3* was used for RNA-Seq in this study) under LN or HN supply. down, down-regulated genes; up, up-regulated genes; No Diff, no significant difference. **b** Expression abundances of *OSH15* in WT, *stp28* lines under LN or HN supply. Data are mean ± SD ($n = 5$ biological replicates). **c** OSH15 directly binds to motif regions of *OsGA2ox3/5/8/9* promoter in EMSA. OSH15 binding site was indicated with red triangle in the respectively promoter model. The results are representative of three independent experiments. **d** Transactivation assays. OSH15 displays transcriptional repression activity to *GA2ox3/5/8/9* promoter-LUC in rice protoplasts. Data are mean ± SD ($n = 9$ biological replicates. Significant difference was determined by two-sided Student's *t*-test. **e** Expression abundance of *OsGA2ox3/5/8/9* in WT and *osh15* lines under LN or HN supply. Data are mean ± SD ($n = 4$ biological replicates). **f**–**h**, GA2ox activities (**f**), phenotype (**g**) and tiller number (**h**) and of WT and *osh15* lines under LN or HN supply. In **f**, **h**, boxes show the first quartile, median, and third quartile; whiskers show the minimum and maximum values. $n = 4$ biological replicates in (**f**), and $n = 9$ individual plants in (**h**). Scale bar, 20 cm. In (**b**, **e**, **f**, **h**), Different letters indicated significant differences ($P < 0.05$, one-way ANOVA, Tukey's HSD test).

To understand the molecular mechanism of OsSTP28-regulated TRN in rice, it is important to address the question how OSH15 is repressed by N supply or by knockout of *OsSTP28*. Given that OsSTP28 largely determines the glucose level in tiller buds, we thought that the repression of *OSH15* under HN supply or in *stp28* mutant might be relate to the effect of glucose signal. Indeed, we found that many components of glucose signaling pathway such as *OsHKXs* and *OsTOR* were remarkably activated upon HN supply or in *stp28* mutant, while carbon deficiency regulators *OsSnRKs* were obviously suppressed at the same conditions, indicating that glucose signal is activated by N supply or by knockout of *OsSTP28* in rice (Supplementary Fig. 18a, b). Recently, it has been reported that glucose signal causes epigenetic silencing of many key genes by activating PRC2-facilitated trimethylation of histone H3 at Lysine 27 (H3K27me3) in plants[28]. Interestingly, *KNOX* (an orthologue of *OSH15* in Arabidopsis) is also found to be silenced by H3K27me3 modification[29]. Thus, it is possible that glucose-dependent epigenetic silencing might inhibit *OSH15* expression during the response of tillering to N. By remining the epigenome data in rice[30] via ChIP-Hub algorithm[31], we found a strong H3K27me3 signal at the coding sequence of *OSH15*, especially within its first three exons (Supplementary Fig. 18c), implying that *OSH15* has been regulated by epigenetic silencing in rice. Then, we conducted a H3K27me3-specific chromatin immunoprecipitation PCR (ChIP-PCR) assay and found that the H3K27me3 modification of *OSH15* was significantly enhanced by HN supply in WT or by the knockout of *OsSTP28* irrespective of N condition (Supplementary Fig. 18d), which fully explained the silencing of *OSH15* at the same conditions (Fig. 5b). Altogether, we propose that H3K27me3-related epigenetic modification silences *OSH15* expression during OsSTP28-mediated TRN.

Next, we verified whether the elevated apoplastic glucose in *stp28* mutants or under HN supply intermediates the impact of OsSTP28 on *OSH15-OsGA2oxs* module to regulate tillering. For this purpose, we supplied 2% glucose to WT rice in order to mimic the response of apoplastic glucose to N input or *OsSTP28* knockout. It showed that the external glucose supplementation significantly stimulated tillering in rice, and consistently *OSH15* expression was repressed while *OsGA2oxs* expression and GA2-oxidase activity were enhanced at the same situation (Supplementary Fig. 19). In addition, 2-Deoxy-d-Glucose (2-DG), a competitive glycolytic inhibitor, was supplied together with glucose to WT rice. Interestingly, the supply of 2-DG did not weaken but even slightly enhanced the effect of glucose on *OSH15* expression, *OsGA2oxs*-mediated GA catabolism, and tillering (Supplementary Fig. 19), suggesting that glucose itself rather than glycolysis acts as a signal to regulate *OSH15-OsGA2oxs* module thus impacting tillering in rice.

Elite allele of *OsSTP28* contributes to improvement of N-responsive yield formation and N use efficiency in rice

We carried out field experiment to investigate the contribution of OsSTP28 in the improvement of yield and NUE in rice production. Among the three determinants of grain yield, the panicle number as a direct reflection of tillering was largely improved in *stp28* mutants compared with WT under both LN and HN supplies (Supplementary Fig. 20a, b; Fig. 6a, b). Meanwhile, the grain number per panicle or grain weight was not increased even reduced at the limited N condition in *stp28* mutants (Supplementary Fig. 20c, d; Fig. 6c, d), which might reflect a tradeoff of the boosting tillering in *stp28* mutants.

As a consequence, due to the largely enhanced tillering (panicle number), inactivation of *OsSTP28* resulted in increase of grain yield and NUE by about 20–21% under LN condition and by about 10-13% under HN condition (Supplementary Fig. 20e, f; Fig. 6e, f). The results confirm that tillering enhancement makes a major contribution to the improvement of rice yield and NUE in response to increased N fertilizer input[2,3,7], and demonstrate that OsSTP28 plays critical role in regulating TRN and yield formation, especially when N application is limited. Moreover, the complementation of $OsSTP28^{Hap.\ H}$ allele achieved a higher panicle number, grain yield, and NUE compared with that of $OsSTP28^{Hap.\ C}$ allele under HN supply (Fig. 6a, b, e, f), demonstrating that the elite $OsSTP28^{Hap.H}$ allele is a valuable germplasm for the genetic improvement of N-responsive yield formation and NUE in rice.

Furthermore, we address the question whether the modulation of TRN in rice by OsSTP28 is independent of OsTCP19. First, we found that the allelic variation between *OsTCP19-H* and *OsTCP19-L* did not alter TRN in our four-parent MAGIC population (Supplementary Fig. 21a–c). Since the negative transcriptional response of *OsTCP19* to N supply endows OsTCP19 with the ability to module N-induced tillering[7], we monitored *OsTCP19* expression pattern in *stp28* mutants. As shown, N-inhibited expression pattern of *OsTCP19* was unaffected by the knockout of *OsSTP28* (Supplementary Fig. 21d), and N-repressed expression of OsSTP28 was unchanged in the *ostcp19* mutant compared with its WT either (Supplementary Fig. 21e). These data strongly suggested that OsSTP28 and OsTCP19 works independently with each other in rice. Interestingly, the elite allele *OsTCP19-H* has almost been lost in modern Asian cultivated rice varieties, especially in those accessions developed in N-rich region[7]. By contrast, the elite $OsSTP28^{Hap.\ H}$ allele was highly distributed in Asian cultivated rice (Supplementary Fig. 3), thus implying a possible complementary occurrence of the $OsSTP28^{Hap.H}$ allele to that of *OsTCP19-H*. To test this hypothesis, we re-sequenced *OsTCP19* and *OsSTP28* alleles in 18 modern elite japonica rice varieties that are currently used for rice production in Jiangsu Province (a temperate and N-rich region in China). Indeed, all 18 modern elite japonica rice varieties contain the weak allele *OsTCP19-L*, while 17 of them contains the elite $OsSTP28^{Hap.H}$ allele (Supplementary Fig. 21f). Among these 18 modern elite japonica rice varieties, the tillering and yield response was still quite sensitive to increased N fertilizer input (Supplementary Fig. 21g). Thus, the elite allele $OsSTP28^{Hap.H}$ is likely to complement the declination of *OsTCP19* to modulate N-responsive tillering and yield formation in modern elite japonica rice varieties mainly developed and cultivated in N-rich region.

In addition, the expression response of *OsSTP28* to N was negatively correlated with TRN in these tested rice varieties (Supplementary Fig. 21i), indicating a potential breeding strategy to improve N-responsive tillering and yield via suppressing the transcript abundance of *OsSTP28*. Indeed, knockout of *OsSTP28* in several elite Asian cultivated rice such as MH63 (Ming Hui 63, containing $OsSTP28^{Hap.\ C}$ allele) and GLA4 (Guang Lu Ai 4, containing $OsSTP28^{Hap.\ H}$ allele) by genome editing substantially improved their N-responsive tillering and grain yield (Fig. 6g, h; Supplementary Fig. 22). Taken together, our study reveals that *OsSTP28* is a vital genetic locus with large potential to improve rice yield and NUE in agricultural production by coordinating phytohormone metabolism with N fertilizer input.

Discussion

The genetic basis and molecular mechanism of tillering response to N and yield formation are inherently complex. It has been shown that a transcription factor OsTCP19 contributes to geographical adaptation of rice tillering response to diverse soil N content[7]. The elite allele *OsTCP19-H* is enriched in rice varieties originating from N-deficient regions (such as wild rice or *aus* rice varieties) and has been lost in most modern cultivated rice varieties. However, modern elite rice cultivars used in current rice production still exhibits high sensitivity to achieve N-induced tillering (Supplementary Fig. 21g), implying that a OsTCP19-independent pathway is required to modulate tillering response to N. Indeed, our study shows that OsSTP28 functions independent of OsTCP19 (Supplementary Fig. 21a–e). More importantly, the elite allele $OsSTP28^{Hap.\ H}$ displays a higher frequency in modern cultivated rice, thus showing a complementary occurrence compared with *OsTCP19-H* (Supplementary Fig. 3). These data suggest that OsSTP28 facilities a OsTCP19-independent regulatory cascade to

https://doi.org/10.1038/s41467-024-53651-1

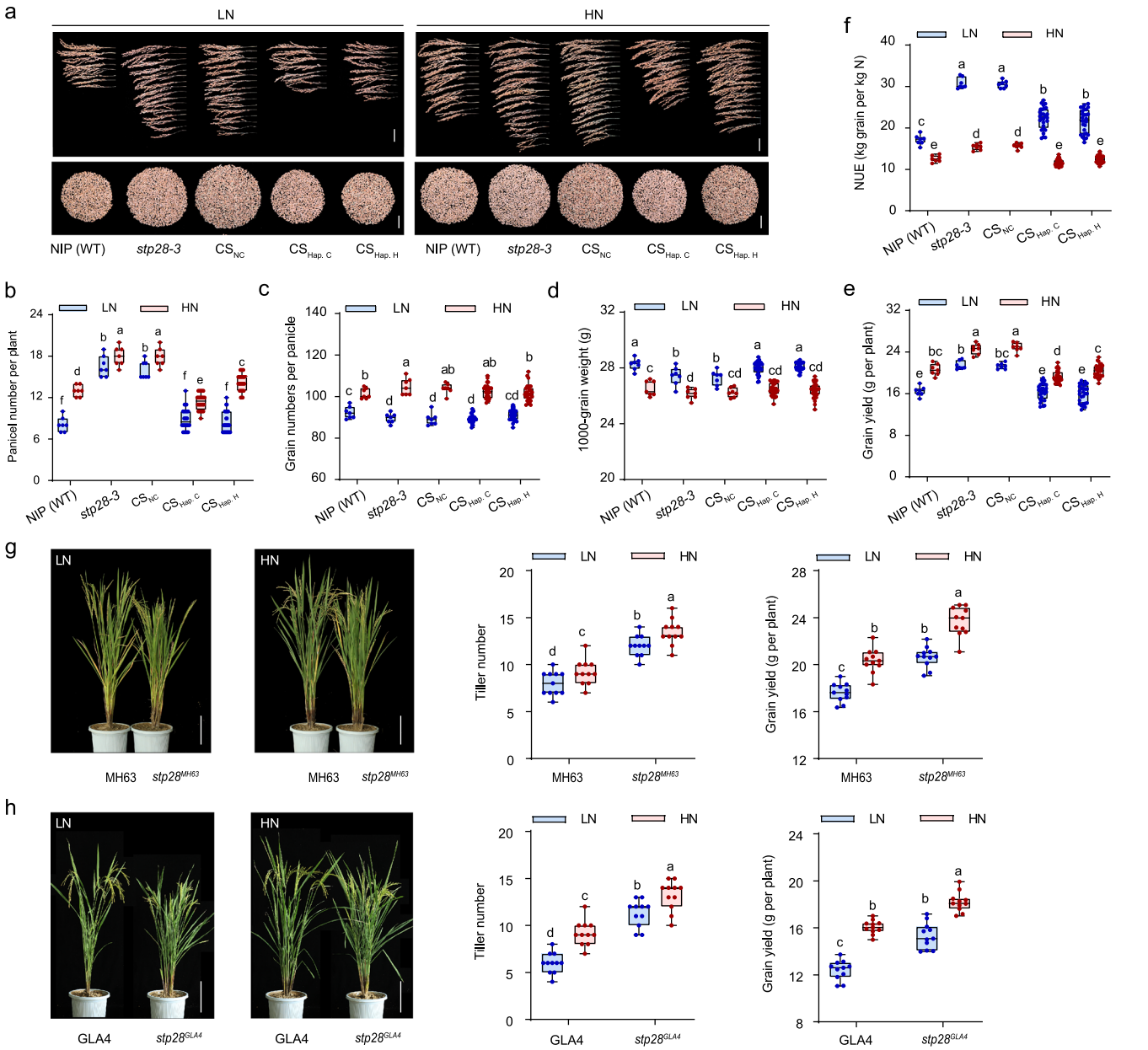

Fig. 6 | Elite allele of *OsSTP28* contributes to improvement of N-responsive yield formation and N use efficiency in rice. a–e Phenotype (**a**), panicle number (**b**), grain number per panicle (**c**), 1000-grain weight (**d**), yield per plant (**e**) and N use efficiency (NUE) (**f**) in WT, *stp28-3*, CS_{NC}, $CS_{Hap.C}$ and $CS_{Hap.H}$ at mature stage under LN or HN supply in Nanjing in 2023. Scale bar = 3.5 cm in (**a**). Four independent $CS_{Hap.C}$ and $CS_{Hap.H}$ complementation lines were tested in this study. Accordingly, in (**b**–**f**), boxes show the first quartile, median, and third quartile; whiskers show the minimum and maximum values. $n = 7$ individual plants for WT, *stp28-3*, and CS_{NC}; $n = 28$ individual plants for $CS_{Hap.C}$ and $CS_{Hap.H}$. Different letters indicate significant differences at $P < 0.05$ according to one-way ANOVA and Tukey's HSD test. **g, h** Phenotype, tiller number and grain yield per plant in MH63 (Ming Hui 63, containing $OsSTP28^{Hap.C}$ allele) and $stp28^{MH63}$ lines (**g**), or in GLA4 (Guang Lu Ai 4, containing $OsSTP28^{Hap.H}$ allele) and $stp28^{GLA4}$ lines (**h**) under LN or HN supply. Scale bar = 20 cm in (**g**, **h**). In (**g**, **h**), boxes show the first quartile, median, and third quartile; whiskers show the minimum and maximum values. $n = 11$ individual plants. Different letters indicate significant differences at $P < 0.05$ according to one-way ANOVA and Tukey's HSD test.

complement the declination of *OsTCP19* and module N-responsive tillering in modern elite rice varieties which are mainly selected and cultivated in N-rich regions (Supplementary Fig. 21f, h). Moreover, the negative correlation between the expression response of *OsSTP28* and the tillering response to N in current elite rice cultivars used in China suggests that reducing the expression of *OsSTP28* may represent a practical breeding strategy for rice yield and NUE improvement.

Green revolution in rice originates from the discovery and application of serious allelic mutations of *semi-dwarf1 (sd1)* that causes defects on GA biosynthesis and reduces the abundance of bioactive GA[32,33]. Thus, GA pathway is tightly linked with rice productive and NUE in particularly after green revolution[2,6]. Previous study demonstrates that GA signaling pathway and its downstream component NGR5 play a critical role in achieving N-responsive tillering in rice[11]. Upon elevated N availability, NGR5 is stabilized by DELLA proteins to trigger rice tillering. However, it remains unclear how the signal of N availability is integrated into GA-NGR5 pathway to regulate tiller development. In present study, we find that OsSTP28 acts as a critical intermediator to transduce the signal of N availability to coordinate GA catabolism with tillering response to N in rice. In response to increased N supply, suppressed expression of *OsSTP28* leads to the activation of GA2oxs-facilitated GA catabolism in shoot base, which reduces the content of

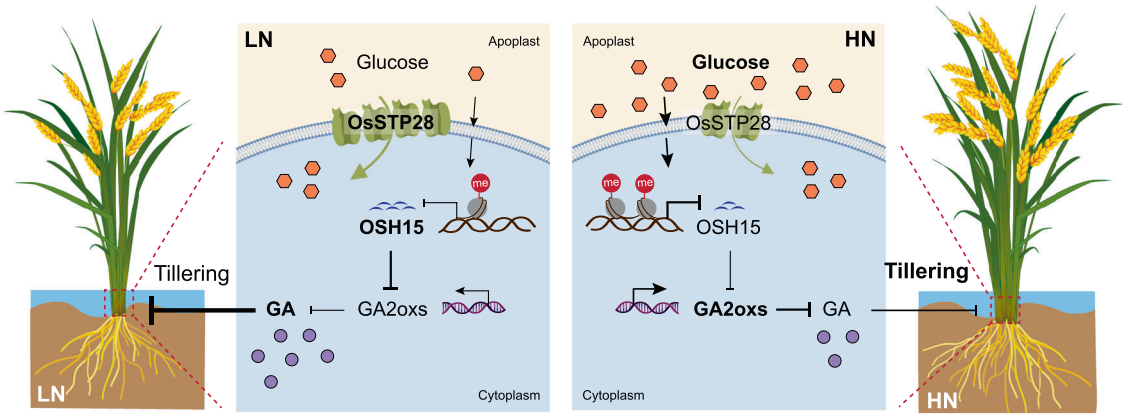

Fig. 7 | Working model of *OsSTP28*-glucose mediated tillering pathway. N supply negatively regulates the expression of *OsSTP28* to generate glucose accumulation in tiller buds, which in turn silences the expression of a transcriptional factor *OSH15* via H3K27me3 modification to active GA2-oxidases catalyzed GA catabolism in shoot base. OsSTP28-OSH15-GA2oxs module reduces the level of bioactive gibberellin in shoot base under increased N supply, and consequently stimulates tillering.

bioactive GAs and consequently promotes tillering (Fig. 4). This impact of OsSTP28 on GA catabolism depends on the involvement of a transcription inhibitor OSH15 that can directly bind to the promoter of *GA2oxs* to negatively regulate GA catabolism (Fig. 5). Intriguingly, OSH15 binding site, TGAC motif, is widely existed in the promoters of *GA2oxs* across gramineous species, and similarly, KNOTTED1, an orthologue of OSH15 in maize, is also able to directly repress *GA2oxs* expression[34], suggesting that the regulation of OSH15 on GA catabolism is likely a conserved mechanism across gramineous species. Furthermore, genetic analysis verified that OsSTP28 functions upstream of GA catabolism and NGR5 to modulate N-responsive tillering (Fig. 4h–j; Supplementary Fig. 16e, f). Taken together, OsSTP28-OSH15-GA2oxs represents an important entry point of the environmental N availability to coordinate GA-NGR5 pathway with tiller development in rice.

Sugar is an important regulator of shoot branching/tillering across many plant species[35]. Previous studies elucidate that elevated sugar content in shoot base where tiller buds are generated can promote tiller outgrowth in rice[16,36]. In agreement with this point, we observed an accumulation of glucose in the shoot base of rice under high N supply (Fig. 3g, h; Supplementary Fig. 8), and the supplementation of external glucose stimulate tiller bud outgrowth (Supplementary Fig. 19a, b). Note that, sugar homeostasis in plants is tightly associated with photoperiod. Carbon dioxide is fixed by photosynthesis to generate sucrose and starch in the light period; whereas starch and sucrose are degraded into glucose and fructose to maintain respiration in the dark period[37]. In particular, apoplast sucrose is hydrolyzed by cell wall invertase to produce glucose then imported into sink tissues by STPs[38]. This explains why the N-responsive expression of *OsSTP28* and accumulation of glucose are taken place at night (Fig. 3; Supplementary Fig. 8). Considering that OsSTP28 facilitates glucose influx, the inactivation of *OsSTP28* either by increasing N supply or by knockout of *OsSTP28* leads to the accumulation of apoplastic glucose which functions as a signal to stimulating tillering in rice (Fig. 3h). Meanwhile, we have not detected significant difference of intracellular glucose between HN and LN or between WT and *stp28* mutant (Supplementary Fig. 9). However, it is still a big challenge to precisely detect glucose level in the cytoplasm. Recently, OsSTP15, an orthologue of OsSTP28, has also been reported as a regulator of tillering in rice[36]. Compared with *OsSTP28*, we found *OsSTP15* was insensitive to N supply (Supplementary Fig. 6b). OsSTP15 modules tillering by impacting cytokinin (CK)[36], seems not by impacting GA pathway. These differences between OsSTP15 and OsSTP28 suggest that OsSTP15 is more likely to be a general regulator of tillering, while OsSTP28 is a vital player of N-responsive tillering. Nevertheless, our study highlights that OsSTP28 serves as a critical checkpoint to coordinate an appropriate balance between N availability and carbohydrate distribution that is essential for achieving N-responsive tillering and yield formation in rice.

Since the influence of glucose on OSH15-GA2oxs mediated GA catabolism and tillering does not rely on the glucose metabolic process (Supplementary Fig. 19), we consider that glucose acts likely as a signal to coordinate GA catabolism with N-responsive tillering. To evaluate the influence of glucose on OsSTP28-mediated TRN, we further dissected the expression of several key components in glucose signaling pathway by transcriptome analysis. It is clearly shown that the glucose signal is activated by increasing N input or by knockout of *OsSTP28* in shoot base (Supplementary Fig. 18a), which is consistent with the enhanced tillering at the same conditions (Fig. 2c–e; Supplementary Fig. 5). Although the mechanism in sensing apoplastic glucose level needs to be uncovered, the glucose signal in plant can activate PRC2 complex in a TOR kinase-dependent manner to promoter H3K27 methylation which suppresses many gene expression[28]. Our data demonstrate that N-induced and OsSTP28-related silencing of *OSH15* in rice is due to the activated H3K27me3 modification (Supplementary Fig. 18c, d). Interestingly, *KNOX* an orthologue of *OSH15* in Arabidopsis also undergo a H3K27me3-related epigenetic silencing[29]. It seems that H3K27me3 modification functions as a conserved epigenetic mechanism to modulate the expression of *KNOX-like* transcription factor across the plant kingdom.

In summary, our study demonstrates that OsSTP28 functions as a key regulator to achieve N-responsive tillering and yield formation in rice (Fig. 7). External N input negative regulates the expression of *OsSTP28* to cause an accumulation of glucose in tiller buds. Then, the elevated glucose signal silences *OSH15* via H3K27me3 modification to release the expression of GA2oxs that coordinates GA catabolism to boost tillering. Moreover, an elite allele of *OsSTP28* with higher sensitivity to N supply or inactivation of *OsSTP28* are able to promote N-responsive tillering and yield formation effectively in modern cultivated rice varieties, thus providing a gene resource and the strategy to the genetic improvement of yield and NUE for the sustainable rice production.

Methods

Plant materials

120 lines of MAGIC population were developed via four-way cross by using HHZ5-SAL9-Y3-Y1 (HH), PR33282-B-8-1-1-1-1-1 (PR), SAGC-08 (SA) and BP1976B-2-3-7-TB-1-1 (BP) as the parent varieties[15].

Oryza sativa (ssp. Japonica. cv. Nipponbare) was used as wild-type rice in this study. *stp28* mutants (*stp28-1*, *stp28-2* and *stp28-3*), *osh15* mutants (*osh15-1* and *osh15-2*) and *ga2ox5* mutants (*ga2ox5-1*, *ga2ox5-2* and *ga2ox5-3*) were generated in the Nipponbare (NIP) background by CRISPR/Cas9 technology.

To generate *OsSTP28* complementation lines, the coding sequence of *OsSTP28* from NIP under the control of different promoters (2600 bp-$OsSTP28^{Hap.\ C}$ from SA; 2600 bp-$OsSTP28^{Hap.\ H}$ from HH) was introduced into *stp28-3* mutant via infection with A. tumefaciens strain EHA105.

To knockout *OsSTP28* in the elite cultivated rice varieties, $stp28^{GLA4}$ and $stp28^{MH63}$ mutants were generated in the background of GLA4 (Guang Lu Ai 4, *indica* rice) and MH63 (Ming Hui 63, *indica* rice) by CRISPR/Cas9 system.

18 modern elite *japonica* rice varieties used for current rice production in Jiangsu Province were provided by Prof. Jie Yang (Jiangsu Academy of Agricultural Sciences, Nanjing, China).

Plant growth conditions

For paddy field experiments, rice seedlings were cultivated in Baima field in Nanjing (119° 18′E, 31° 61′N) under long-day conditions (13.5 h day) from May to October. Rice seeds were sown in May and nurtured for 30 days in seed beds before being transplanted to paddy fields, where they grew until the harvest stage in October. The plant spacing between each seedling was 15 cm, and 7 plants per row × 8 rows for each replicate of the treatment were planted with at least 3 replicates under LN (150 kg N/ha) or HN (350 kg N/ha) conditions. Urea as the only N source was applied at seedling, tillering and heading stage, which respectively accounted for 50%, 25% and 25% of the total N. After 3 months of growth, tiller number and yield characters were analyzed in harvest stage. All field trials were repeated for at least two years.

For hydroponic experiments, plants were cultivated in a growth chamber with photocycles of 14 h (30 °C) and 10 h (28 °C), humidity of about 70%, and photon density of about 200 μmol m^{-2} s^{-1}. IRRI nutrient solution was used for hydroponics culture[17]. After 4 days of germination, rice seedling was transferred into 1/4 IRRI nutrient solution for 3 days, cultured in 1/2 IRRI nutrient solution for 3 days and then in IRRI nutrient solution for 7 days. 0.125 mM and 1.25 mM NH_4NO_3 were used for LN and HN treatments, respectively. The nutrient solution was changed daily. At the end of day or at the start of the day, seedling was harvest for phenotype observation or for physiological analyses.

Genome-wide association analysis

A satisfactory normal distribution of tillering was observed in 120 accessions of MAGIC population in present study. A mixed linear model was employed to conduct association analysis of the data[39]. A *q*-value cutoff of 0.05 was used as the threshold to determine the significant association. Horizontal solid line on the Manhattan plot indicates the genome-wide significance threshold $q \le 0.05$. The Manhattan plot was obtained from the analysis with software TASSEL v5.0 and drawn using the R package[40].

Plastid construction and plant transformation for gene editing

All small guide RNA (sgRNA) used for CRISPR/Cas9-facilitated genome editing in this study were designed by CRISPR-PLANT (http://omap.org/crispr/jbrowse/), and all sgRNA sequences are listed in Supplementary Data 5. All plasmids were transformed into rice via A. tumefaciens strain *EHA105*. The genotypes of transgenic rice lines were confirmed by DNA sequencing.

Quantitative reverse transcription PCR

For the *OsSTP28* expression assay, blades, sheaths, shoot bases and roots were sampled at the end of night. To determine the rhythmic expression of *OsSTP28*, the shoot bases of rice seedlings were sampled every 4 h for 2 d. To investigate the response of *OsSTP28* to N, rice seedlings were cultivated in a hydroponic system under LN or HN supply for 7 d, and the shoot bases were sampled. For the *OSH15 and GA2ox3/5/8/9* expression assay, shoot bases were sampled at the end of night. Every sample was consisted of a mixture of 7 plants. Samples were frozen in liquid nitrogen immediately and well ground, and then total RNA was extracted using Trizol reagent (Cat. #15596018, Thermo Fisher Scientific, MA, USA) according to the manufacturer's instructions. RNA concentrations were measured using Nanodrop 2000plus (Thermo Fisher Scientific Inc., MA, USA). cDNA synthesis was performed using ReverTra Ace®qPCR RT Master Mix with gDNA Remover (Cat. #FSQ-301, TOYOBO LIFE SCI., Shanghai, China). The qRT-PCR reactions were prepared using SYBR Green Master Mix (Cat. #Q111, Vazyme Bio, Nanjing, China) following the manufacturer's protocol, and carried out by using a thermal cycler equipped with an QuantStudio™ Real-Time PCR Software system (ABI QuantStudio3, Thermo Fisher Scientific Inc., MA, USA). Transcript levels were normalized to the *OsActin1* gene (*Os03g0718100*), and expression values were calculated using the $2^{-\Delta Ct}$ method with the geometric mean of the Ct values of *Actin1* as a reference. Gene-specific primers are listed in Supplementary Data 5.

RNA-seq analysis

Shoot bases (~0.5 cm) of rice from WT and *stp28-3* were harvested under LN or HN supply. According to rhythmic fluctuation of glucose, the maximal difference of glucose between wild type and *stp28* mutant was detected at the end of night, thus the samples for RNA-seq were harvested at this time point. RNA extraction was performed using the RNeasy Micro Kit (Cat. #74004, Qiagen, Germany). RNA integrity and purity were assessed using 1% agarose gels to monitor degradation and contamination. RNA purity was checked using the NanoDrop® 2000plus (Thermo Fisher Scientific Inc., MA, USA). RNA integrity was assessed using the RNA Nano 6000 Assay Kit of the Bioanalyzer 2100 system (Agilent Technologies, CA, USA). The cDNA libraries were sequenced on the Illumina sequencing platform by BGI (Shenzhen, China). Clean reads were compared to oryza_sativa_Ensembl_52 (ftp://ftp.ensemblgenomes.org/pub/plants/release-52/fasta/oryza_sativa/dna/). DESeq2 v1.22.1 was used to analyze the differential expression between the two groups, and the *P* value was corrected using the Benjamini & Hochberg method. The corrected *P* value and $|\log_2 foldchange|$ are used as the threshold for significant difference expression. Data analysis and graphing were conducted by R (ggplot).

RNA in situ hybridization of *OsSTP28* and histological staining

RNA in situ hybridizations were carried out as the description by Luo[41]. 14-old-seedling rice shoot bases were harvested from the hydroponic system at the end of the night and fixed in FAA solution ((Solarbio LIFE SCIENCES, G2355). Thin sections of paraffin-embedded shoot bases of 8–12 μm thickness were generated for the hybridization. A 121 bp-length cDNAs of *OsSTP28* was selected for synthesis of digoxigenin (DIG)-labeled RNA sense and antisense probes in vitro by DIG RNA Labeling Kit (SP6/T7) (Cat. #1175025, Roche Applied Science, Basel, Switzerland). The hybridization reaction was conducted for 24 h at 50 °C. Anti-DIG alkaline phosphatase-conjugated antibody and the NBT (nitro-blue tetrazolium)/ BCIP (5-bromo-4-chloro-3-indolyl phosphate) staining method were used to visualize the tissue-specific localization of *OsSTP28* expression in shoot base sections. Photographs were taken by Axio Scope A1 microscope.

For histochemical analysis of *proOsSTP28:GUS* reporter line, the native promoter sequence (2600 bp) of *OsSTP28* was amplified from Nipponbare genomic DNA by PCR, linked with the GUS gene to generate *OsSTP28* promoter-GUS construct. The construct was then transformed into rice (cv. Nipponbare) via Agrobacterium-mediated transformation. The roots, basal nodes, leaf sheaths and leaf blades of five independent transgenic rice seedlings were incubated with a GUS reaction mix at 37 °C for 1 h. The samples were decolorized bradytely

with anhydrous ethanol, and imaged with an Olympus BX-51microscope equipped with a DC Vie digital camera.

Subcellular localization analysis of OsSTP28

Subcellular localization of OsSTP28 was detected using the full-length cDNA sequence of *OsSTP28* fused in-frame into the pSAT6A-EGFP-N1 vector driven by the 35S promoter. Rice protoplasts were isolated from NIP sheaths. Total 10 μg plasmids (pSAT6A-EGFP, OsRac1-mCherry (a plasma membrane control) and/or STP28-GFP and OsRac1-mCherry) were respectively transformed into rice protoplasts by the polyethylene-glycol-mediated method. Then after incubated in the dark for 12–15 h at 28 °C, a confocal laser scanning microscope (TCS SP8X, Leica; Germany) was used to observe the fluorescence signals in transformed protoplasts at 488 nm/498–540 nm for eGFP and 552 nm/600–640 nm for mCherry.

Heterologous expression of *OsSTP28* in yeast and *X. laevis* oocytes

For yeast assay, *OsSTP28* coding sequence was inserted into the PDR196 vector, containing the ampicillin-resistance gene, and then transferred into the sugar transporter-deficient yeast strain EBY.VW4000. A single clone of EBY.VW4000 containing OsSTP28 was precultured on maltose–amino acid medium [0.67% (w/v) yeast nitrogen base, 1% (w/v) casamino acids, 0.002% (w/v) tryptophan and 2% (w/v) maltose] to an A600 of 0.8–1.0, then the growth of EBY.vw4000 expressing OsSTP28 was assessed on culture media containing 2% concentrations of different sugars (maltose, glucose, fructose, galactose and xylose). Yeast growth phenotype was recorded after 3 days of cultivation.

For oocyte assay, *OsSTP28* coding sequence (CDS) was cloned into pT7Ts vector. The plasmid was then linearized and purified (Cycle-Pure Kit, Cat. #D6492, OMEGA). Capped cRNAs of *OsSTP28* were synthesized using mMESSAGE mMACHINE T7 (Cat. #AM1340; USA), and subsequently, 25–50 ng of cRNAs were injected into healthy-looking oocytes isolated from Xenopus laevis. The incubation of injected oocytes followed the described method. For glucose efflux assay, 10-20 incubated oocytes were transferred into MBS solution supplied respectively with 0-, 2-,20-, 40- and 60-mM [^{13}C]-glucose (Shanghai Engineering Research Center of Stable Isotope, CAS: 492-62-6) for 2 h. For glucose influx assay, 0-, 2- and 20-mM D-glucose was respectively injected into oocytes, and those oocytes was incubated on MBS solution for 2 h. And then, cold MBS buffer was used to wash the oocytes 5 times after incubation at 20 °C, cells were transferred to ice-cold Na-Ringer, washed three times, solubilized with 100 μl 1% (w/v) SDS, and finally measured individually.

Glucose, fructose and sucrose measurements

To investigate the rhythmic fluctuation of sugar in rice shoot bases, 35-d-old seedlings of WT and *stp28* mutants were harvested every 4 h for 2 d. To determine sugar response to N, shoot bases and leaves were respectively stripped from rice seedlings of WT and *stp28* mutants at the end of the night and/or at the end of the day. Every sample was mixed with 9 plants. All samples were freeze-dried for 4 days and ground into powder, and then 0.2 g of dry sample was weighed into 10 ml tubes. Subsequently, 2 ml of 80% ethanol was added to each tube, and the mixture was sonicated at 80 °C for 10 min. The supernatant was absorbed after centrifuge 11,500 g × 5 min. 1 ml of 50% ethanol was added to the precipitate, and the supernatant was taken by ultrasonic at 80 °C for 10 min and 11,150 g × 5 min. The supernatant was combined into a new centrifuge tube and extracted by adding an equal volume of chloroform. The supernatant was taken into the new centrifuge tube at 11,150 g × 5 min. Under the condition of 35 °C, the nitrogen blower quickly dried; 50% acetonitrile was added to 1 ml, and then filtered through 0.45 μm microporous membrane for HPLC determination. The standard curve was prepared with glucose, sucrose and fructose standards. The samples were determination using high performance liquid chromatography (HPLC) (Waters Associates, MA, USA).

Assay of ^{13}C-radiolabeling glucose

The fully unfolded leaves of mutants and WT were fed with water containing 2% [^{13}C]-glucose (produced by Shanghai Engineering Research Center of Stable Isotope, CAS: 492-62-6) for 10 h. The rice was grown in the IRRI nutrient solution (Tang et al., 2012). Subsequently, the leaves, sheaths, shoot bases, and roots were collected and dried at 105 °C for 1 h. Dry materials were ground into powder and weighed using a Beckman LS650. At least three biological replicates were analyzed using Isotope Ratio Mass Spectrometry (IRMS, Thermos Fisher Scientific, MA, USA).

Apoplastic and intracellular sugar measurements

Plant apoplast space can be divided into air- and solution-volume. After being treated in different N conditions for 7 days and washed in pure water, samples were weighed as an initial volume (M0). The samples were vacuumed in pure water by the injector and weighed as M1. Ectoplasmic solution after centrifuge 4500 g × 10 min at 4 °C was collected and weighed as M2. The apoplast space (M0, M1 and M2) was calculated by using a method of Gentzel[42]. The concentration of extracted sucrose, glucose and fructose was determined by ultra performance liquid chromatography (UPLC) (Hclass, Waters, USA).

To determine the levels of intracellular sugar, the protoplast solution was isolated by centrifugation. Briefly, after low-speed centrifugation, apoplastic solution was thrown out from the rice tissue. The remaining rice tissue was cleaned by H_2O and dried by airing. After centrifugation at 12,000 g for 20 min, the supernatant was collected for intracellular sugar determination by UPLC (Hclass, Waters, USA).

Transient transactivation assay in rice leaf protoplast

The full-length *OSH15* coding sequence was cloned into pGreenII-62-sk vector. ~3000 bp upstream sequence (including promoter sequencing and UTR) of *OsGA2ox3/5/8/9* coding region were amplified as the respective promoter. Rice leaf protoplast of two-week-old seedlings was extracted as a method described by Zhang[17]. Each upstream sequence was fused with firefly luciferase (LUC) sequences and introduced to pGreenII-0800 vector to generate the reporter construct. Plasmids containing the effector and reporter vectors were transfected into rice protoplast. After 12 h of infiltration under dark conditions at 30 °C, protoplast proteins were extracted for the detection of Renilla luciferase (REN) and LUC activities using the Double-Luciferase Reporter Assay Kit (Cat. #FR201, TransGen Biotech, Beijing, China). Protoplasts without transfection (water only) and protoplasts transfected with the reporter vector only (empty) were used as negative controls.

Electrophoretic mobility shift assays

Full-length CDS of *OSH15* was cloned into pET-29a (+) vector which was transformed into BL21 strain of Escherichia coli to express fusion protein. The promoter sequence of OsGA2ox3/5/8/9 was selected containing about 100 bp up- and down-stream of the "gatgacctga" motif. Bio-probes were synthesized with biotin labels at both their 3′ and 5′ ends, while the fragment without biotin served as a cold probe. A nondenatured polyacrylamide gel was prepared and subjected to electrophoresis, and color development was achieved using film. All the primers used for probes and competitors are listed in Supplementary Data 5.

Rice endogenous GAs analysis

The shoot bases of NIP and *stp28* lines were collected at the tillering stage under both LN and HN conditions, immediately frozen in liquid nitrogen, and ground into powder. The method of determination of

endogenous GAs was carried out according to previous reports[43]. Briefly, plant samples (100 mg FW) and spiked isotope-labeled internal standards (IS) (D2-GAs, 1 ng) were extracted with 90% MeOH (1 ml) overnight at 4 °C. The extract was then centrifuged at 12,000 g for 15 min at 4 °C and the supernatant was collected. The crude extracts were loaded onto the connected MCX–WAX cartridges and analyzed by UPLC–MS/MS (Hclass, Waters, USA).

Determination of GA2-oxidases activities

GA2-oxidases activities of the tissues (the same as those used for endogenous GAs analysis) were determined with the GA2-oxidases Kit (HuaBang BIO, HB-P5974Z) following the manufacturer's instructions.

H3K27me3 modification analysis

The ChIP-PCR experiments were carried out as previously described with slight modifications[44]. Briefly, 2 g of rice shoot bases were collected and ground into a fine powder using liquid nitrogen. The powdered tissue was incubated with a nuclei isolation buffer for 20 min. Chromatin was fixed using 1% formaldehyde for 10 min, and then the crosslinking reaction was terminated by adding fresh-prepared glycine. The chromatin was then sonicated using the M220 Focused Ultrasonicator (Covaris, USA) to obtain DNA fragment of ~350 bp in size. Immunoprecipitation was performed with 3 µl (1 mg/ml) of anti-H3K27me3 (A2363, ABclonal) at 4 °C overnight. Following this, 30 µl of Magnetic Protein A/G Dynabeads (Invitrogen™, 10002D) were added, and the mixture was incubated at 4 °C for 4 h. The slurry was subjected to a serial of washes using low salt buffer (150 mM NaCl), high salt buffer (500 mM NaCl), and LiCl wash buffer (10 mM Tris-HCl, pH 8.0, 1 mM EDTA, 0.25 M LiCl, 1% Nonidet P-40, 1% sodium deoxycholate). Crosslinks were reversed by incubating the sample at 65 °C overnight. Finally, the precipitated DNA was purified and quantified by qPCR with the primers listed in Supplementary Data 5.

Statistical analysis

Data were collected by Microsoft Excel 2021. All collected data were analyzed using GraphPad Prism 8 (version 8.3.0). Two-tailed Student's *t*-test, Dunnett's multiple test, or Tukey's HSD test was performed to test the statistical significance, and the *P* values of each statistical analysis are noted in figure legends. Graphs were plotted by GraphPad Prism 8 (version 8.3.0) and edited by Adobe Illustrator 2020 (version 24.2.1).

Accession numbers

Sequence data from this study can be found in the GeneBank data libraries or The Rice Annotation Project (RAP) under the following accession numbers: *OsSTP28* (Os11g0594000); *OsGA2ox3* (Os01g0757200); *OsGA2ox5* (Os07g0103500); OsGA2ox8 (Os05g0560900); OsGA2ox9 (Os02g0630300); *OSH15* (Os07g0129700); *NGR5* (Os05g0389000); *OsTCP19* (Os06g0226700); *MOC1* (Os06g0610350); *OsMADS57* (Os02g0731200); *OsTB1* (Os03g0706500); *OsSPL14* (Os08g0509600); *D14* (Os03g0203200); *D3* (Os06g0154200); *D53* (Os11g0104300); *D27* (Os11g0587000); *D17* (Os04g0550600); and *D10* (Os01g0746400). The accession number of differentially expressed genes shown in Supplementary Fig. 11f, Supplementary Fig. 12b and Supplementary Fig. 18b are listed in Supplementary Data 6.

Reporting summary

Further information on research design is available in the Nature Portfolio Reporting Summary linked to this article.

Data availability

The RNA-seq data generated in this study have been deposited in the NCBI (National Center for Biotechnology Information) database under accession code PRJNA1070824. The analysis data of RNA-seq and primers generated in this study are provided in the Supplementary Data 1–5. For any datasets unavailable through the links above, they can be requested from the corresponding author. Source data are provided with this paper.

References

1. Xu, G., Fan, X. & Miller, A. J. Plant nitrogen assimilation and use efficiency. *Annu Rev. Plant Biol.* **63**, 153–182 (2012).
2. Liu, Q. et al. Improving crop nitrogen use efficiency toward sustainable green revolution. *Annu. Rev. Plant Biol.* **73**, 523–551 (2022).
3. Hu, B., Wang, W., Chen, J., Liu, Y. & Chu, C. Genetic improvement toward nitrogen-use efficiency in rice: Lessons and perspectives. *Mol. Plant* **16**, 64–74 (2023).
4. Guo, J. H. et al. Significant acidification in major Chinese croplands. *Science* **327**, 1008–1010 (2010).
5. Sutton, M. A. et al. Too much of a good thing. *Nature* **472**, 159–161 (2011).
6. Luo, L., Zhang, Y. & Xu, G. How does nitrogen shape plant architecture? *J. Exp. Bot.* **71**, 4415–4427 (2020).
7. Liu, Y. Q. et al. Genomic basis of geographical adaptation to soil nitrogen in rice. *Nature* **590**, 600–605 (2021).
8. Wang, Y. & Li, J. Branching in rice. *Curr. Opin. Plant Biol.* **14**, 94–99 (2011).
9. Takai, T. Potential of rice tillering for sustainable food production. *J. Exp. Bot.* **75**, 708–720 (2023).
10. Luo, L., Pan, S., Liu, X., Wang, H. & Xu, G. Nitrogen deficiency inhibits cell division-determined elongation, but not initiation, of rice tiller buds. *Isr. J. Plant Sci.* **64**, 32–40 (2017).
11. Wu, K. et al. Enhanced sustainable green revolution yield via nitrogen-responsive chromatin modulation in rice. *Science* **367**, 6478 (2020).
12. Hou, M. et al. OsPIN9, an auxin efflux carrier, is required for the regulation of rice tiller bud outgrowth by ammonium. *N. Phytol.* **229**, 935–949 (2021).
13. Zhuang, L. et al. Gibberellic acid inhibition of tillering in tall fescue involving crosstalks with cytokinins and transcriptional regulation of genes controlling axillary bud outgrowth. *Plant Sci.* **287**, 110168 (2019).
14. Liao, Z. et al. SLR1 inhibits MOC1 degradation to coordinate tiller number and plant height in rice. *Nat. Commun.* **10**, 2738 (2019).
15. Meng, L., Guo, L., Ponce, K., Zhao, X. & Ye, G. Characterization of three rice multiparent advanced generation intercross (MAGIC) populations for quantitative trait loci identification. *Plant Genome* **9**, 2 (2016).
16. Wang, F. et al. The rice circadian clock regulates tiller growth and panicle development through strigolactone signaling and sugar sensing. *Plant Cell* **32**, 3124–3138 (2020).
17. Zhang, S. et al. Nitrogen mediates flowering time and nitrogen use efficiency via floral regulators in rice. *Curr. Biol.* **31**, 671–683 (2021).
18. Marchive, C. et al. Nuclear retention of the transcription factor NLP7 orchestrates the early response to nitrate in plants. *Nat. Commun.* **4**, 1713 (2013).
19. Hu, B. et al. Nitrate-NRT1.1B-SPX4 cascade integrates nitrogen and phosphorus signalling networks in plants. *Nat. Plants* **5**, 401–413 (2019).
20. Zhao, H. et al. An inferred functional impact map of genetic variants in rice. *Mol. Plant.* **14**, 1584–1599 (2021).
21. Deng, X. et al. A novel insight into functional divergence of the MST gene family in rice based on comprehensive expression patterns. *Genes* **10**, 239 (2019).
22. Schleucher, J., Vanderveer, P. J. & Sharkey, T. D. Export of carbon from chloroplasts at night. *Plant Physiol.* **118**, 1439–1445 (1998).
23. Li, X. et al. Control of tillering in rice. *Nature* **422**, 618–621 (2003).
24. Guo, S. Y. et al. The interaction between OsMADS57 and OsTB1 modulates rice tillering via DWARF14. *Nat. Commun.* **4**, 1566 (2013).

25. Takeda, T. et al. The OsTB1 gene negatively regulates lateral branching in rice. *Plant J.* **33**, 513–520 (2003).
26. Jiao, Y. et al. Regulation of OsSPL14 by OsmiR156 defines ideal plant architecture in rice. *Nat. Genet.* **42**, 541–544 (2010).
27. Lo, S. F. et al. A novel class of gibberellin 2-oxidases control semidwarfism, tillering, and root development in rice. *Plant Cell* **20**, 2603–2618 (2008).
28. Ye, R. et al. Glucose-driven TOR-FIE-PRC2 signalling controls plant development. *Nature* **609**, 986–993 (2022).
29. Xu, L. & Shen, W. H. Polycomb silencing of KNOX genes confines shoot stem cell niches in Arabidopsis. *Curr. Biol.* **18**, 1966–1971 (2008).
30. Zhao, L. et al. Integrative analysis of reference epigenomes in 20 rice varieties. *Nat. Commun.* **11**, 2658 (2020).
31. Fu, L. Y. et al. ChIP-Hub provides an integrative platform for exploring plant regulome. *Nat. Commun.* **13**, 3413 (2022).
32. Sasaki, A. et al. Green revolution: a mutant gibberellin-synthesis gene in rice. *Nature* **416**, 701–702 (2002).
33. Spielmeyer, W. et al. Isolation of gibberellin metabolic pathway genes from barley and comparative mapping in barley, wheat and rice. *Theor. Appl. Genet.* **109**, 847–855 (2004).
34. Bolduc, N. & Hake, S. The maize transcription factor KNOTTED1 directly regulates the gibberellin catabolism gene *ga2ox1*. *Plant Cell* **21**, 1647–1658 (2009).
35. Wang, B., Smith, S. M. & Li, J. Genetic regulation of shoot architecture. *Annu. Rev. Plant Biol.* **69**, 437–468 (2018).
36. Li, M. et al. Knockout of the sugar transporter OsSTP15 enhances grain yield by improving tiller number due to increased sugar content in the shoot base of rice (Oryza sativa L.). *N. Phytol.* **241**, 1250–1265 (2024).
37. Lemoine, R. et al. Source-to-sink transport of sugar and regulation by environmental factors. *Front. Plant Sci.* **4**, 272 (2013).
38. Slewinski, T. L. Diverse functional roles of monosaccharide transporters and their homologs in vascular plants: a physiological perspective. *Mol. Plant* **4**, 641–662 (2011).
39. Zhou, X. & Stephens, M. Genome-wide efficient mixed-model analysis for association studies. *Nat. Genet.* **44**, 821–824 (2012).
40. Bradbury, P. J. et al. TASSEL: software for association mapping of complex traits in diverse samples. *Bioinformatics* **23**, 2633–2635 (2007).
41. Luo, L. et al. Developmental analysis of the early steps in strigolactone-mediated axillary bud dormancy in rice. *Plant J.* **97**, 1006–1021 (2019).
42. Gentzel, I., Giese, L., Zhao, W., Alonso, A. & Mackey, D. A simple method for measuring apoplast hydration and collecting apoplast contents. *Plant Physiol.* **179**, 1265–1272 (2019).
43. Xin, P., Guo, Q., Li, B., Cheng, S., Yan, J. & Chu, J. A tailored high-efficiency sample pretreatment method for simultaneous quantification of 10 classes of known endogenous phytohormones. *Plant Commun.* **1**, 100047 (2020).
44. Xu, Y. et al. Arabidopsis MRG domain proteins bridge two histone modifications to elevate expression of flowering genes. *Nucleic Acids Res.* **42**, 10960–10974 (2014).

Acknowledgements

We thank Prof. Yufeng Wu and Dr. Le Luo (Nanjing Agricultural University) for the help with GWAS analysis and RNA in situ hybridization, Prof. Jie Yang (Jiangsu Academy of Agricultural Science) for providing modern elite *japonica* rice varieties, Prof. Bin Hu (South China Agricultural University) for providing *tcp19-1* and *tcp19-2* rice mutants, Prof. Mingjun Li (Northwest A&F University) for providing yeast strain EBY.VW4000 and Dr. Fengying Duan (Chinese Academy of Agricultural Sciences) for the technical help with the measurement of apoplastic sugars, Dr. Dijun Chen and Tao Zhu (Nanjing University) for the help of remining the epigenome data in rice. This study is supported by National Key Research and Development Program of China (2021YFF1000400), National Natural Science Foundation of China (31930101), Jiangsu Provincial Key Research and Development Program (BE2020339), Jiangsu Seed Industry Revitalization Project (JBGS [2021] 011) with grants to G.X., and by Jiangsu Provincial Key Research and Development Program (BE2022336) with a grant to Y.L.

Author contributions

G.X., Y.L., and J.Z. conceived the project and designed the experiments. J.Z. performed most of the experiments and data analysis, Y.Z. helped with the biochemistry experiments. J.C., M.X., and X.G. helped with the field experiments, C.W. and Y.X. performed ChIP-PCR assay to detect H3K27me3 modification, J.C. helped with endogenous GAs measurement, S.Z., H.Q., M.G. helped with data analysis and graphs plotting. G.X., Y.L., and J.Z. wrote the manuscript with the support from all authors. All authors contributed to the finalization of the manuscript.

Competing interests

The authors declare no competing interests.

Additional information

Supplementary information The online version contains supplementary material available at https://doi.org/10.1038/s41467-024-53651-1.

Correspondence and requests for materials should be addressed to Ying Liu or Guohua Xu.

Peer review information *Nature Communications* thanks Jian Jin, Zuofeng Zhu and the other, anonymous, reviewers for their contribution to the peer review of this work. A peer review file is available.